

Impacts of mechanistic changes on HO_x formation and recycling in the oxidation of isoprene

A. T. Archibald^{1,*}, M. C. Cooke¹, S. R. Utembe¹, D. E. Shallcross¹, R. G. Derwent², and M. E. Jenkin^{1,3}

¹School of Chemistry, University of Bristol, Bristol, BS8 1TS, UK

²rdscientific, Newbury, Berkshire, RG14 6LH, UK

³Atmospheric Chemistry Services, Okehampton, Devon, EX20 1FB, UK

* now at: NCAS-Climate, Department of Chemistry, University of Cambridge, Cambridge CB2 1EW, UK

Received: 14 January 2010 – Published in Atmos. Chem. Phys. Discuss.: 1 March 2010

Revised: 13 August 2010 – Accepted: 18 August 2010 – Published: 1 September 2010

Abstract. Recently reported model-measurement discrepancies for the concentrations of the HO_x radical species (OH and HO₂) in locations characterized by high emission rates of isoprene have indicated possible deficiencies in the representation of OH recycling and formation in isoprene mechanisms currently employed in numerical models; particularly at low levels of NO_x. Using version 3.1 of the Master Chemical Mechanism (MCM v3.1) as a base mechanism, the sensitivity of the system to a number of detailed mechanistic changes is examined for a wide range of NO_x levels, using a simple box model. The studies consider sensitivity tests in relation to three general areas for which experimental and/or theoretical evidence has been reported in the peer-reviewed literature, as follows: (1) implementation of propagating channels for the reactions of HO₂ with acyl and β-oxo peroxy radicals with HO₂, with support from a number of studies; (2) implementation of the OH-catalysed conversion of isoprene-derived hydroperoxides to isomeric epoxydiols, as characterised by Paulot et al. (2009a); and (3) implementation of a mechanism involving respective 1,5 and 1,6 H atom shift isomerisation reactions of the β-hydroxyalkenyl and cis-δ-hydroxyalkenyl peroxy radical isomers, formed from the sequential addition of OH and O₂ to isoprene, based on the theoretical study of Peeters et al. (2009). All the considered mechanistic changes lead to simulated increases in the concentrations of OH, with (1) and (2) resulting in respective increases of up to about 7% and 16%, depending on the level of NO_x. (3) is found to have potentially much greater impacts, with enhancements in OH concentrations of up to a factor of about 3.3, depending on the level of NO_x,

provided the (crucial) rapid photolysis of the hydroperoxy-methyl-butenal products of the cis-δ-hydroxyalkenyl peroxy radical isomerisation reactions is represented, as also postulated by Peeters et al. (2009). Additional tests suggest that the mechanism with the reported parameters cannot be fully reconciled with atmospheric observations and existing laboratory data without some degree of parameter refinement and optimisation which would probably include a reduction in the peroxy radical isomerisation rates and a consequent reduction in the OH enhancement propensity. However, an order of magnitude reduction in the isomerisation rates is still found to yield notable enhancements in OH concentrations of up to a factor of about 2, with the maximum impact at the low end of the considered NO_x range.

A parameterized representation of the mechanistic changes is optimized and implemented into a reduced variant of the Common Representative Intermediates mechanism (CRI v2-R5), for use in the STOCHEM global chemistry-transport model. The impacts of the modified chemistry in the global model are shown to be consistent with those observed in the box model sensitivity studies, and the results are illustrated and discussed with a particular focus on the tropical forested regions of the Amazon and Borneo where unexpectedly elevated concentrations of OH have recently been reported.

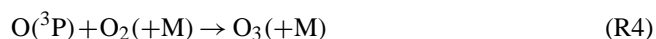
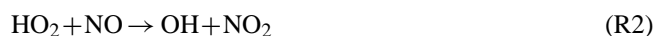
1 Introduction

The role of the hydroxyl radical (OH) as initiator in the degradation of volatile organic compounds (VOCs) in the troposphere has been well established for several decades and has led to the species being termed the atmospheric



Correspondence to: M. E. Jenkin
(atmos.chem@btinternet.com)

“cleanser” (Heard and Pilling, 2003). In the presence of nitrogen oxides (NO_x = NO + NO₂) it has long been recognized that the reactions of OH with VOCs can initiate rapid sequences of reactions, in which organic peroxy radicals (RO₂), oxy radicals (RO) and the hydroperoxy radical (HO₂) can act as chain propagating species, leading to the regeneration of OH (e.g., Lightfoot et al., 1992; Jenkin and Clemitshaw, 2000). The reactions of RO₂ and HO₂ with NO play a key role in these catalytic cycles, since the associated oxidation of NO to NO₂ leads to the formation of ozone following the subsequent photolysis of NO₂:



In the absence of high levels of NO_x, the reactions of RO₂ with HO₂ have generally been accepted to play an important role in traditional understanding of the chemistry of VOC oxidation, leading to chain termination and a general suppression of the concentrations of the free radical species:



However, analysis of recent direct measurements of OH and HO₂ (collectively referred to as HO_x) over the Amazonian rainforest (Lelieveld et al., 2008) and the tropical forests of Borneo (Pugh et al., 2010a) have suggested that, in the absence of high levels of NO_x, there must be an unknown recycling mechanism for OH, as the current chemistry employed in numerical model studies cannot reproduce the measurements. Moreover, these findings are not just limited to the tropics. One can see that a clear pattern arises of model underestimation for OH that is linked primarily with the collocation of isoprene emissions (Tan et al., 2001; Thornton et al., 2002; Martinez et al., 2003; Ren et al., 2008).

This issue has recently been addressed in the global modelling study of Butler et al. (2008) and constrained box modelling study of Kubistin et al. (2008), which have shown that model-measurement discrepancies related to the GABRIEL campaign over the Amazonian rainforest can be reconciled by artificially increasing the extent of OH recycling at low NO_x, through a parametric adjustment to Reaction (R5) for isoprene-derived RO₂ radicals, in which *n* molecules of OH are added to the reaction products. Optimised values of *n* = 2 and *n* = 3.2 were reported by Butler et al. (2008) and Kubistin et al. (2008), respectively. Although the representation is artificial, some support derives from the results of a number of recent laboratory studies, which have demonstrated that several oxygenated RO₂ radicals possess radical-propagating channels for their reactions with HO₂. (Hasson et al., 2004; Jenkin et al., 2007, 2008a, 2010; Dillon and Crowley, 2008).

Kubistin et al. (2008) also examined whether this conclusion could be explained by a variety of novel (but related) chemical pathways, including enhanced photolysis of the organic hydroperoxide (ROOH) products and competitive photolysis of the RO₂ radicals themselves, but no single chemically feasible pathway was found. However, a recent theoretical study of Peeters et al. (2009) has suggested that some of the isomeric isoprene-derived RO₂ radicals can undergo unimolecular isomerisation reactions that are estimated to be competitive with the bimolecular reactions, such as Reaction (R5), which are usually considered to dominate under low NO_x conditions. In conjunction with the resultant production of particularly photolabile unsaturated hydroperoxyaldehyde products, Peeters et al. (2009) postulated that this chemistry could be a major factor in reconciling the reported model-measurement discrepancies. In addition to this, the further OH-initiated oxidation of the hydroperoxide (ROOH) products, formed in Reaction (R5), has recently been shown to proceed predominantly via an OH-neutral pathway involving OH-catalysed conversion into isomeric epoxydiols (Paulot et al., 2009a), thereby potentially removing an OH sink in many mechanistic representations of isoprene degradation.

Recently, Pugh et al. (2010a) have also highlighted the need for accurate characterization and representation of physical processes in addressing model-measurement discrepancies, in relation to measurements made as part of the OP3 campaign in Malaysian Borneo. In part they conclude that air mass segregation effects for OH and isoprene (as also proposed by Butler et al., 2008) potentially play an important role, based on investigating the impact of phenomenological reductions in the rate coefficient for the reaction of OH with isoprene, which were reported to be as high as 50%. The model-measurement discrepancies may therefore have contributions from shortcomings in the representation of both chemistry and dynamics. However, a more recent assessment of segregation effects in the OP3 campaign has suggested a substantially smaller impact than previously reported (Pugh et al., 2010b), which is more comparable to the 15% phenomenological reduction in rate coefficient reported recently by Dlugi et al. (2010), based on measurements over a deciduous forest in Germany.

The aim of the present paper is specifically to address the impacts of detailed chemical mechanistic changes on the formation and recycling of HO_x during the oxidation of isoprene. The paper is split into two parts, with the first part being dedicated to investigating the fine details of this chemical system over a wide range of NO_x levels, using sensitivity tests involving the Master Chemical Mechanism version 3.1 (MCM v3.1) and a simple box model. MCM v3.1 provides an explicit reaction framework of elementary reactions (described in Sect. 2), which is ideally suited as a benchmark for testing detailed mechanistic changes. It was also applied in the studies of Lelieveld et al. (2008), Butler et al. (2008) and Kubistin et al. (2008) either directly, or by virtue of being

The peroxy radicals (RO₂ and HO₂) thus provide the coupling with the chemistry of NO_x, which leads to NO-to-NO₂ conversion, and formation of O₃ upon photolysis of NO₂ (via Reactions R3 and R4). The subsequently-formed oxy radicals determine the identities of the carbonyl products generated from the degradation. In MCM v3.1, the β-hydroxyalkenyloxy radicals, ISOPBO and ISOPDO, are assumed to undergo exclusive C-C bond scission, leading to the formation of HCHO and the well-established C₄ carbonyl products, methacrolein (MACR) and methylvinyl ketone (MVK), resulting in respective molar yields of about 68%, 22% and 34% from the NO_x-propagated chemistry, in good agreement with those reported in the literature (e.g., Calvert et al., 2000 and references therein). On the basis of the results of Ruppert and Becker (2000) and Yu et al. (1995), a minor decomposition channel is also included for ISOPBO, leading to the formation of hydroxymethylvinyl ketone (MVKOH) with a molar yield of about 11%, as shown in Fig. 1, although it is noted that this process is not supported by the results of Benkelberg et al. (2000).

The δ-hydroxyalkenyloxy radicals, ISOPAO and ISOPCO, are assumed to generate the closely-related C₅ hydroxycarbonyl products 4-hydroxy-2-methyl-but-2-enal (HC4CCHO) and 4-hydroxy-2-methyl-but-2-enal (HC4ACHO), which have also been reported in the literature (Calvert et al., 2000; Zhao et al., 2004; Baker et al., 2005; Paulot et al., 2009b). In MCM v3.1, this is assumed to occur in each case via a 1,5-H atom shift isomerisation, followed by reaction of the resulting α-hydroxy organic radical with O₂, in agreement with the appraisals of Zhao et al. (2003) and Park et al. (2004). It should be noted that the same products would be formed (albeit from the alternative oxy radical) if ISOPAO and ISOPCO reacted directly with O₂. As shown in Fig. 1, the resultant total molar yield of C₅ hydroxycarbonyl products from the NO_x-propagated chemistry is about 22%, in reasonable agreement with that reported (Calvert et al., 2000; Zhao et al., 2004; Baker et al., 2005; Paulot et al., 2009b).

The chemistry discussed above, and represented in reaction sequence Reactions (R6)–(R9) and (R2), consists entirely of propagation reactions which conserve the radical population. Although that chemistry dominates when NO_x is present, some radical removal occurs as a result of the alternative terminating channels for the reactions of the peroxy radicals with NO, which form the corresponding organic nitrate product, e.g.:



As indicated by the total nitrate product yields shown in Fig. 1, the weighted average branching ratio, $k_{7b}/(k_{7a}+k_{7b})$ for first generation nitrate product formation in MCM v3.1 is assigned a value of 10%, based on an evaluation of reported yields (e.g., see Pinho et al., 2005), such that the suite of oxy radicals (ISOPAO, ISOPBO, ISOPCO and ISOPDO) is formed from the propagating chemistry with a yield of

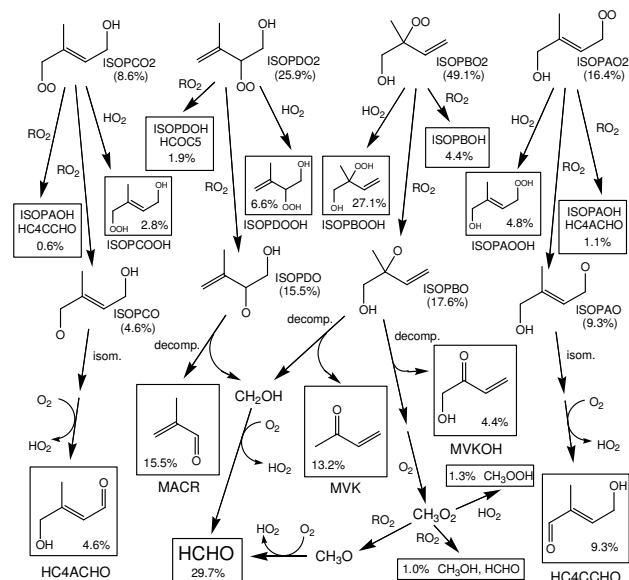
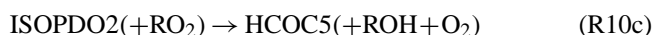


Fig. 2. MCM v3.1 representation of the OH initiated degradation of isoprene to first generation products, in the absence of NO_x (routes to formation of initial peroxy radicals are as shown in Fig. 1). Species names correspond to those appearing in MCM v3.1. Closed-shell products are displayed in boxes, along with their molar yields (N.B., HCHO, HC4ACHO and HC4CCHO are generated by more than one displayed reaction, such that their respective total molar yields are 30.7%, 5.8% and 9.9%). The yields correspond to conditions representative of traditional NO_x-free chamber experiments with no primary HO₂ source (see text).

90%. It is noted that reported laboratory determinations of the yields of isoprene nitrates from the OH-initiated chemistry show some variability, although the more recent studies report values lying in the range 7–12% (Sprengnether et al., 2002; Patchen et al., 2007; Paulot et al., 2009b; Lockwood et al., 2010). The value applied in MCM v3.1 is therefore consistent with these determinations, and is also in agreement with the recent recommendation of the IUPAC data evaluation panel (IUPAC, 2010).

The OH-initiated degradation chemistry to first generation products when NO_x is absent, as represented in MCM v3.1, is summarized in Fig. 2. Under these conditions, removal of the peroxy radicals occurs either via parameterized “permutation reactions” with the “pool” of available organic peroxy radicals (denoted “RO₂”), or via reaction with HO₂. e.g.:



Of these reactions only Reaction (R10a) is propagating, such that the formation of the suite of oxy radicals (ISOPAO, ISOPBO, ISOPCO and ISOPDO) is substantially reduced to a total yield of less than 50% (see Fig. 2); with the balance mainly due to the formation of the hydroperoxide products, in particular ISOPBOOH. It should also be noted that the conditions considered here are representative of NO_x-free laboratory studies which have traditionally been applied to study isoprene degradation, in which HO₂ is formed only as a secondary radical in the system following further reactions of oxy radicals, e.g., from ISOPDO (formed in channel Reaction R10a) via Reactions (R8) and (R9). The product yields displayed for the carbonyl, hydroperoxide and alcohol products in Fig. 2 thus represent such conditions, and generally agree well with those reported (e.g., Ruppert and Becker, 2000; Benkelberg et al., 2000; Lee et al., 2005). Under atmospheric conditions, the reactions of the peroxy radicals with HO₂ tend to be even more significant, such that the first generation MCM v3.1 chemistry predicts substantial radical termination through formation of hydroperoxide products when NO_x levels are low. It is noted, however, that the lifetimes of the peroxy radicals with respect to reaction with HO₂ (and RO₂) can be substantial (e.g., minutes) at the low concentrations which prevail in the atmosphere, such that unimolecular reactions can potentially become more competitive. This is considered further in the sensitivity tests described below (Sect. 3.4).

As outlined by Saunders et al. (2003) and Pinho et al. (2005), the further degradation of the major C₄ and C₅ carbonyl and hydroxycarbonyl products in MCM v3.1 is treated rigorously, and leads ultimately to the generation of CO and CO₂ via a number of well-established intermediate carbonyl products, such as hydroxyacetone (CH₃C(O)CH₂OH), methyl glyoxal (CH₃C(O)CHO), glycolaldehyde (HOCH₂CHO), glyoxal (CH(O)CHO) and additional HCHO. In the presence of sufficient NO_x, the chemistry is propagated by catalytic cycles similar to that presented above for the first generation chemistry, with chain terminating reactions of RO₂ with HO₂ similarly becoming competitive as levels of NO_x decrease. In MCM v3.1, these reactions are fully terminating, and currently do not reflect the results of a number of recent laboratory studies, which have demonstrated that selected oxygenated RO₂ radicals possess significant radical-propagating channels for their reactions with HO₂: (Hasson et al., 2004; Jenkin et al., 2007; 2008a; 2010; Dillon and Crowley, 2008). This has been found to be particularly important for the acetyl peroxy radical (CH₃C(O)O₂), with the product channel:



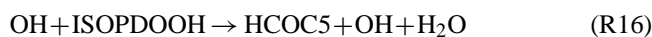
accounting for about 40–50% of the overall reaction (Hasson et al., 2004; Jenkin et al., 2007; Dillon and Crowley, 2008). In addition to CH₃C(O)O₂, the MCM v3.1 chemistry generates a number of other acyl peroxy radicals (i.e.,

of generic formula RC(O)O₂), the reactions of which with HO₂ are also likely to possess significant propagating channels, by analogy. These include the methacryloyl peroxy radical (formed from methacrolein), and RC(O)O₂ radicals formed from the oxidation of HC₄ACHO, HC₄CCHO and HOCH₂CHO. This issue is considered further in the sensitivity tests described below (Sect. 3.2).

As part of a systematic strategy to limit the size of the MCM, a simplified treatment is applied to the degradation of products which are formed exclusively from the reactions of RO₂ with HO₂ and with the peroxy radical pool (Jenkin et al., 1997; Saunders et al., 2003). As indicated above, hydroperoxides formed from the reactions of RO₂ with HO₂ are predicted to play a significant role in isoprene oxidation at low NO_x levels, and it is timely to examine the impact of the applied simplifications. For primary and secondary hydroperoxides, two representative channels are considered by analogy with the reaction of OH with CH₃OOH (e.g., Vaghjiani and Ravishankara, 1989):



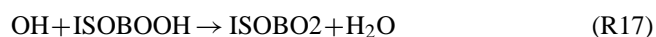
Channel (R13a) is explicit representation of abstraction of the hydroperoxyl H atom, whereas channel (R13b), forming the corresponding carbonyl product and regenerating OH (via removal of a hydrogen atom from the carbon α to the -OOH) is used to represent attack of OH at the organic group. The latter channel is invoked because the carbonyl product (R_{-H}O) is invariably already represented in the mechanism, such that no further expansion in mechanism size is required. If the total rate of attack at the organic group (by all possible pathways) is estimated to exceed the rate of channel (R13a) by more than an order of magnitude (which is the case for all the isoprene-derived hydroperoxides), channel (R13b) is used to represent the entire reaction, with the rate set on the basis of the total estimated reactivity. Consequently, the reactions of OH with the primary and secondary hydroperoxides ISOPAOOH, ISOPCOOH and ISOPDOOH are represented as follows, leading to prompt and quantitative regeneration of OH:



The recent study of Paulot et al. (2009a) has reported strong experimental evidence for prompt, nearly-quantitative OH regeneration, but occurring as part of OH-catalysed conversion of the isoprene-derived hydroperoxides to isomeric epoxydiols. Although yielding different organic products, Reactions (R14)–(R16) are expected to have a similar (effectively neutral) impact on OH as the Paulot et al. (2009a)

mechanism, and this is tested in sensitivity tests described below (Sect. 3.3).

For tertiary hydroperoxides, it is not possible to use channel (R13b) to represent the reaction, owing to the absence of a hydrogen atom on the carbon atom α to the -OOH group. As a result, the entire reaction for all tertiary hydroperoxides in MCM v3.1 is represented by the minor channel type (R13a), with the rate coefficient set on the basis of the total estimated reactivity. This is therefore the case for the major hydroperoxide, ISOPBOOH, formed in MCM v3.1, for which the reaction is thus represented as follows, not regenerating OH:



This representation is clearly a much greater simplification than those applied to the other isoprene-derived hydroperoxides above. In addition to not regenerating OH (in disagreement with the results of Paulot et al., 2009a), Reaction (R17) artificially increases the lifetime of the ISOPBO₂/ISOPBOOH pair, which are interconverted in conjunction with HO_x destruction. The impact of including a detailed representation of the degradation of ISOPBOOH, based on the mechanism of Paulot et al. (2009a), is therefore considered further in the sensitivity tests described below (Sect. 3.3).

3 Box model sensitivity tests using MCM v3.1

3.1 Model set-up and base case simulations

For the mechanistic sensitivity experiments, a 0-D box model using the FACSIMILE kinetics software was applied, as described fully in the recent isoprene mechanism intercomparison of Archibald et al. (2009). The model was designed to simulate a well mixed 1000 m boundary layer, with input parameters representative of tropical regions (Longitude 0.0°, Latitude 3.3° S). Initial mixing ratios of long lived gases were set to concentrations relevant to the tropics: 1.7 ppm CH₄, 100 ppb CO, 30 ppb O₃ and 2 ppb HCHO. The box received emissions of NO and isoprene, which were maintained throughout the model runs. The isoprene emissions were prescribed to vary with temperature and light intensity (Guenther et al., 1995), with an average emission rate of 1.6×10^{12} molecule cm⁻² s⁻¹, which is comparable to surface fluxes reported for tropical regions (Wiedinmyer et al., 2005; Eerdekens et al., 2009). The NO emission rate was held constant throughout the model runs, using a series of rates over the range from 5.0×10^9 molecule cm⁻² s⁻¹ to 1.0×10^{12} molecule cm⁻² s⁻¹. Photolysis coefficients were calculated assuming clear sky conditions, using a parameterization previously applied with the MCM (Jenkin et al., 1997; Saunders et al., 2003). Loss of product species via physical processes (i.e., deposition or transfer to the condensed phase)

was not represented, thereby enabling the results to be interpreted directly in terms of the maximum potential impacts of the considered gas phase chemical mechanistic changes on HO_x radical recycling and formation. In practice, the omission of such processes has a near-zero effect on most of the sensitivity tests presented here, because they mainly relate to the HO_x impacts of processes occurring in the first generation of oxidation, or involving reactions of first-generation products with short lifetimes with respect to gas phase removal.

In agreement with the results of a number of previous studies (as discussed in Sect. 1), the mechanism intercomparison of Archibald et al. (2009) also demonstrated that, at the lowest levels of NO_x and highest levels of isoprene, all the considered mechanisms (MCM v3.1, CRI v2, MIM-2, GEOS-CHEM, MOZART v4, UKCA, CBM-05 and STOCHEM) simulated OH mixing ratios that were considerably smaller than measurements suggest (e.g., Lelieveld et al., 2008). In order to maintain the levels of OH consistent with those that have been observed, Archibald et al. (2009) included an additional dummy source of OH that was related to the light-dependent correction factor for isoprene emissions. In the present study, runs have specifically been carried out without this additional source, to examine whether the mechanistic adjustments described below are able to elevate OH concentrations towards levels that are more consistent with those observed.

Figure 3 shows the results of a series of base case simulations (denoted “Mechanism 0”) performed with the MCM v3.1 chemistry for a selection of key species or species groupings. Similarly to Archibald et al. (2009), we mainly present the arithmetic mean mixing ratios for the species on the second day of the box model run as a function of average NO_x mixing ratio, which covers the range from 42.3 ppt to 10.2 ppb. The simulated NO_x trends show a qualitative similarity to those presented for the same species with MCM v3.1 in Fig. 1 of Archibald et al. (2009) (and discussed in detail in that paper), but with the impact of not including the additional dummy source of OH in the present simulations becoming increasingly apparent towards the low end of the NO_x range. In particular, the mixing ratio for OH simulated here for the lowest input rate of NO_x ([OH] = 6.0×10^{-3} ppt, or about 1.5×10^5 molecule cm⁻³) is approaching an order of magnitude lower than that presented by Archibald et al. (2009), with this leading to correspondingly greater mixing ratios for isoprene, which is controlled mainly by reaction with OH.

In the sections that follow, the impacts of a number of mechanistic sensitivity tests (summarized in Table 1) are presented. As indicated above, these tests aim to consider processes for which experimental and/or theoretical evidence has been reported in the peer-reviewed literature.

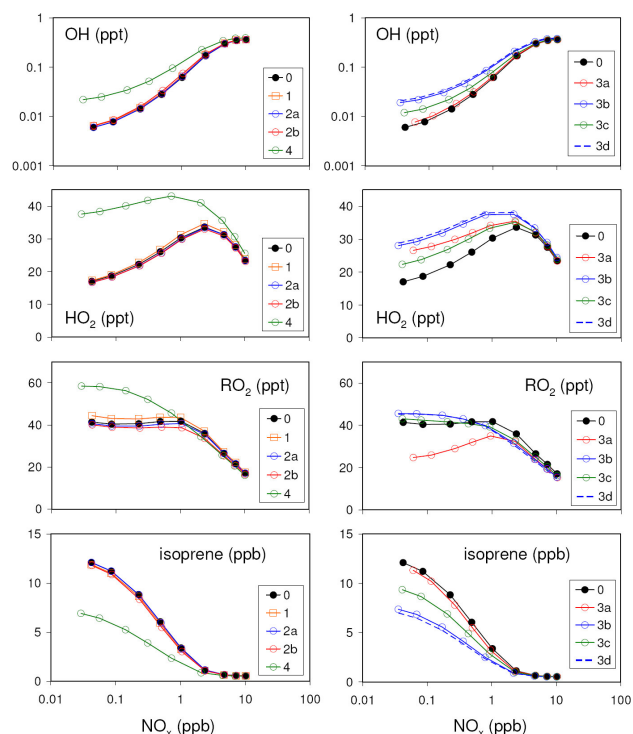


Fig. 3. Simulated mixing ratios of OH, HO₂, RO₂ and isoprene as a function of NO_x mixing ratio, using MCM v3.1 (Mechanism 0) and the mechanism variants described in Table 1. All values are daytime averages on the second day of the simulations, calculated from 06:00 to 18:00 local time in the model.

3.2 Implementation of radical propagating channels for RO₂ + HO₂ reactions

As indicated above in Sect. 2, a number of recent laboratory studies have reported that the reactions of selected oxygenated RO₂ radicals with HO₂ proceed significantly by radical-propagating channels. The MCM v3.1 isoprene chemistry was therefore updated to include such channels for the relevant classes of RO₂ radical for which experimental evidence exists.

On the basis of the results reported for the reaction of HO₂ with the acetyl peroxy radical, CH₃C(O)O₂ (Hasson et al., 2004; Jenkin et al., 2007; Dillon and Crowley, 2008), the reactions of HO₂ with all acyl peroxy radicals of generic formula RC(O)O₂ were updated to include channel (R18c),

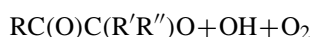


with the branching ratios, based on the recent recommendation of the IUPAC panel for CH₃C(O)O₂: $k_{18a}/k_{18} = 0.41$; $k_{18b}/k_{18} = 0.15$; $k_{18c}/k_{18} = 0.44$ (IUPAC, 2010). The studies

Table 1. Description of main mechanistic sensitivity runs performed (see Sects. 3.2–3.4 and 4).

Mechanism number	Description
0	MCM v3.1
1	MCM v3.1 with radical propagating channels incorporated for all acyl peroxy + HO ₂ and β-oxo peroxy + HO ₂ reactions.
2a	MCM v3.1 with updated chemistry incorporated for the OH-initiated degradation of the primary and secondary hydroperoxides (ISOPAOOH, ISOPCOOH and ISOPDOOH), based on Paulot et al. (2009a).
2b	Mechanism 2a with updated chemistry also incorporated for the OH-initiated degradation of the tertiary hydroperoxide (ISOPBOOH), based on Paulot et al. (2009a).
3a	MCM v3.1 with isomerisation reactions (and associated subsequent chemistry) included for isoprene-derived peroxy radicals, based on Peeters et al. (2009).
3b	Mechanism 3a with enhanced photolysis rate for hydroperoxyaldehyde products, based on Peeters et al. (2009).
3c	Mechanism 3b with rates of isomerisation reactions for isoprene-derived peroxy radicals reduced by a factor of 10.
3d	Mechanism 3b with adjusted rate parameters for isomerisation reactions of the isoprene-derived peroxy radicals, based on Stavrou et al. (2010).
4	A consolidation of the changes outlined above in Mechanisms 1, 2b and 3b.
4R	A reduced representation of Mechanism 4 for use in CRI v2.
4Ra	Mechanism 4R with rates of isomerisation reactions for isoprene-derived peroxy radicals reduced by a factor of 10.

of Jenkin et al. (2008a) and Dillon and Crowley (2008) have shown that the reaction of HO₂ with the simplest β-oxo peroxy radical, CH₃C(O)CH₂O₂, also has a minor radical propagating channel. The reactions of HO₂ with all β-oxo peroxy radicals of generic formula RC(O)C(R'R'')O₂ were therefore also updated to include channel (R19b),



with the branching ratios based on the recent recommendation of the IUPAC panel for CH₃C(O)CH₂O₂:

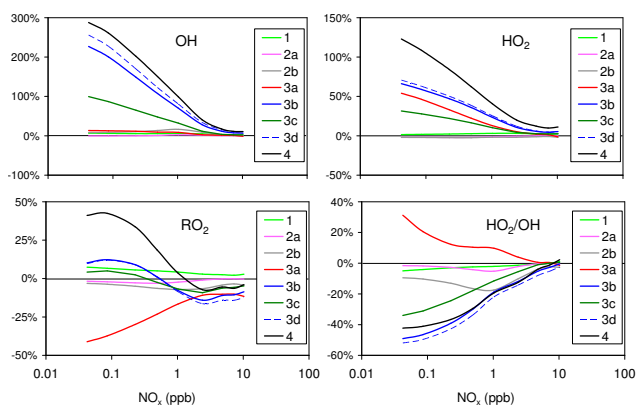


Fig. 4. Changes in mixing ratios of OH, HO₂ and RO₂, and the HO₂/OH ratio, for each mechanistic variant relative to MCM v3.1 (Mechanism 0). Continuous changes as a function of the simulated NO_x level obtained by interpolation of the data shown in Fig. 3.

$k_{19a}/k_{19} = 0.85$; $k_{19b}/k_{19} = 0.15$ (IUPAC, 2010). These combined changes resulted in no new species being formed relative to the base case mechanism and only an increase of 15 in the number of reactions. The resultant mechanism is denoted Mechanism 1 (see Table 1).

The impact of using Mechanism 1, compared with the base MCM v3.1 (Mechanism 0), is shown in Figs. 3 and 4. The changes logically result in generally increased mixing ratios of OH, HO₂ and RO₂, but the effect is small. The simulated increases in OH mixing ratios are about 2% at the high end of the NO_x range (about 10 ppb NO_x), and consistently about 5–7% over the sub-ppb NO_x range. This is consistent with the results of a similar sensitivity test performed by Pugh et al. (2010a) for the conditions of the OP3 campaign in Malaysian Borneo, which resulted in a 4% increase in the peak mixing ratio of OH. The increases in HO₂ mixing ratios are about 2–3% over the entire NO_x range, with those in RO₂ gradually increasing with decreasing NO_x, over the approximate range 2–7% (see Fig. 4).

3.3 Implementation of updated chemistry for first-generation hydroperoxides

As described above in Sect. 2, the OH-initiated degradation of all the hydroperoxide products formed from isoprene in the first generation of degradation is simplified in MCM v3.1, in accordance with protocol rules which were designed to maintain a manageable representation of the intermediates in the degradation of the parent VOCs. Whereas the simplifications applied to the primary and secondary hydroperoxides quantitatively regenerate OH, and are probably a reasonable compromise for those formed in the isoprene system (ISOPAOOH, ISOPCOOH and ISOPDOOH), the simplification for tertiary hydroperoxides is much more severe and may have implications for the representation of the degradation of the major isoprene-derived hydroperoxide, ISOPBOOH.

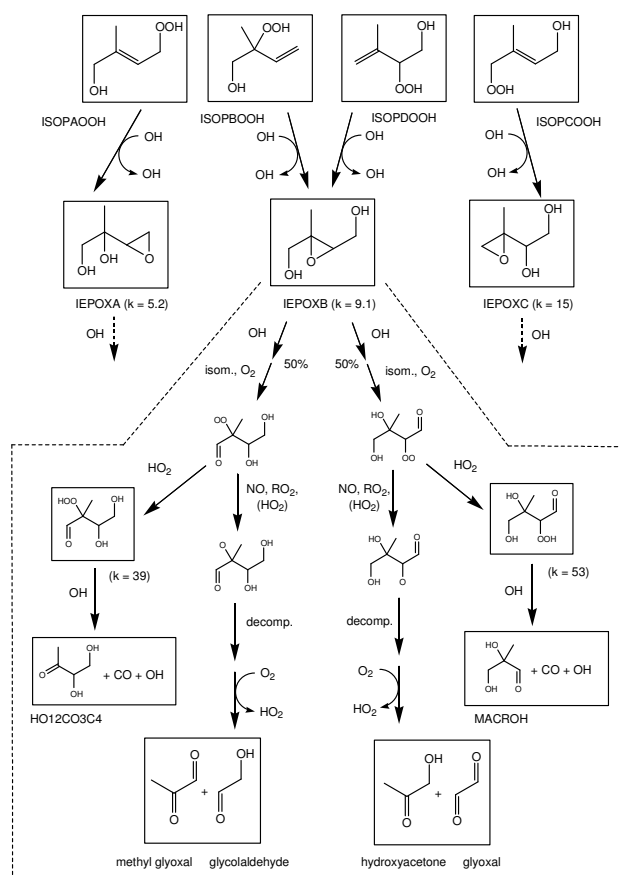


Fig. 5. Schematic representation of the revised OH initiated degradation chemistry of the isoprene-derived hydroperoxides and epoxydiols in Mechanisms 2a and 2b. The chemistry is based on the mechanism of Paulot et al. (2009a), involving initial OH catalysed conversion into epoxydiols (IEPOXA, IEPOXB and IEPOXC). The main features of the further degradation are shown for the major isomer, IEPOXB. Initiation rate coefficients in units $10^{-12} \text{ cm}^3 \text{ molecule}^{-1} \text{ s}^{-1}$. Propagating channels for the reactions of HO₂ with the β -oxo peroxy radicals in this mechanistic extension were only represented in the consolidated Mechanism 4.

The degradation of all the hydroperoxides was updated on the basis of the mechanism of Paulot et al. (2009a), with the major features of the chemistry shown schematically in Fig. 5. The results of Paulot et al. (2009a) suggest that the reactions of OH with the hydroperoxides lead predominantly (90%) to the formation of isomeric epoxydiols, with associated regeneration of OH. In the present sensitivity tests, it is assumed that the reactions proceed exclusively to form the epoxydiols, so the upper limit impact of the mechanism is being assessed. Subsequent explicit degradation chemistry of the epoxydiol isomers was developed on the basis of experimental information provided by Paulot et al. (2009a) for the closely related species, cis-2,3-epoxy-1,4-butanediol, supplemented where necessary by the structure-reactivity method of Kwok and Atkinson (1995), and other

methods as defined in the MCM protocol (Saunders et al., 2003), to estimate rate coefficients and branching ratios. The updated chemistry resulted in an increase of 21 species and 59 reactions relative to the base case mechanism. The resultant mechanism was implemented in two stages, denoted Mechanisms 2a and 2b (see Table 1).

In Mechanism 2a, the chemistry was updated only for the primary and secondary hydroperoxides, ISOPAOOH, ISOPCOOH and ISOPDOOH. As shown in Figs. 3 and 4, the implementation of Mechanism 2a, compared with the base MCM v3.1 (Mechanism 0), has a nearly zero impact on the simulated mixing ratios of OH, consistent with the primary feature being the substitution of one set of OH-neutral reactions with another. However, the secondary impact of the changes to the subsequent degradation mechanism results in small reductions (about 1–3%) in the mixing ratios of HO₂ and RO₂ over the sub-ppb NO_x range.

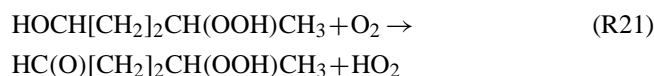
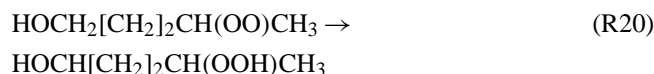
In Mechanism 2b, the chemistry was also updated for the tertiary hydroperoxide, ISOPBOOH. As shown in Figs. 3 and 4, this results in a more notable impact, with increases in the simulated mixing ratios of OH across most of the considered NO_x range. The maximum increase is about 16%, in the middle of the NO_x range, falling to about 8% at the lowest NO_x considered. The unusual NO_x dependence reflects that the impact is due to the removal of the HO_x destruction cycle associated with the representation of ISOPBOOH chemistry in Mechanism 0, which is most efficient when its chain length is greatest. This is determined by a combination of the fraction of OH which reacts with ISOPBOOH, and the fraction of ISOPBO₂ which reacts with HO₂ under the prevailing conditions, which maximises in the centre of the range owing to sufficient suppression of isoprene levels under conditions when ISOPBOOH is still a significant product. The simulated mixing ratios of HO₂ are similar to those obtained with Mechanism 2a, but the simulated RO₂ levels are further reduced (by up to about 6% relative to Mechanism 0) over the entire NO_x range (see Fig. 4).

The results presented here therefore indicate that implementation of the mechanism reported by Paulot et al. (2009a) has a potentially notable impact on simulated OH recycling, but only if the chemistry it is replacing does not already regenerate OH (as is partially the case in MCM v3.1). Given that ISOPBOOH accounts for about 65% of the first-generation isoprene-derived hydroperoxide population in MCM v3.1 (see Fig. 2), it is reasonable to infer from the present results that implementation of the Paulot et al. (2009a) chemistry can potentially increase simulated OH mixing ratios by up to about 25% (depending on NO_x) if it is replacing a representation of hydroperoxide chemistry with zero OH regeneration. Alternatively, if the existing hydroperoxide chemistry is already fully OH-neutral, as is the case in some mechanisms (e.g., CRI v2, as discussed further below in Sect. 4), implementation of the Paulot et al. (2009a) chemistry would likely have a near-zero effect on simulated OH, as the system appears to be much less sensitive to the

details of the subsequent product degradation. However, it is noted that the main and highly significant advance of the Paulot et al. (2009a) study was identification of the formation the epoxydiol co-products and their potential role in secondary organic aerosol (SOA) formation, which is clearly much more sensitive to the classes of product formed in conjunction with OH-neutrality.

3.4 Implementation of isomerisation reactions for RO₂

As levels of NO_x decrease, the removal of the isoprene-derived RO₂ radicals in MCM v3.1 becomes increasingly controlled by their reactions with HO₂ (e.g., Reaction R11), or by parameterized permutation reactions with the pool of available organic peroxy radicals (e.g., Reaction R10). The rate coefficients applied to these reactions have either been measured directly in kinetics studies, or inferred from those measured for reactions of RO₂ radicals possessing close structural similarities (e.g., Jenkin et al., 1998), and the resultant assembly of reactions has been found to give a generally good description of product yields measured in the laboratory for the OH-initiated oxidation of isoprene in the absence of NO_x (e.g., Ruppert et al., 2000). It is recognised, however, that the conditions traditionally applied in laboratory studies are necessarily characterised by concentrations of peroxy radicals which are many orders of magnitude higher than those in the atmosphere, to facilitate reliable quantification of products yields. As a result, the rates of bimolecular second order reactions, such as Reactions (R10) and (R11), are elevated relative to those of any first order processes which might be occurring, such that the product distribution can potentially be unrepresentative of the atmosphere if such first order processes exist. In this respect, Perrin et al. (1998) and Jorand et al. (2003) have reported experimental evidence for the occurrence of 1,6 H atom shift isomerisations of δ-hydroxy peroxy radicals formed during the oxidation of pentane and hexane, leading to the formation of hydroperoxy-carbonyl products, e.g. in the pentane system:



On the basis of extrapolation of higher temperature data, they reported isomerisation rates of about 0.03 s⁻¹ and 0.6 s⁻¹ for the respective shifts of H atoms from a -CH₂OH group and a -CH(OH)- group at 298 K. Should similar rates also be applicable to the isoprene-derived δ-hydroperoxyalkenyl radicals, ISOPAO₂ and ISOPCO₂, the reactions would potentially be competitive with those likely for their reactions with HO₂ or the peroxy radical pool. For

example, in the presence of 50 ppt of HO₂, the loss coefficient for each of the isoprene-derived peroxy radicals via reaction with HO₂ in MCM v3.1 is about 0.02 s⁻¹.

The possible isomerisation of isoprene-derived peroxy radicals possessing both δ-hydroxy and β-hydroxy substituents has recently been addressed as part of the theoretical study of Peeters et al. (2009), who used a combination of DFT and ab initio methods to elucidate potential pathways in the isoprene OH initiated degradation that may be important for the issue of recycling HO_x. Several of the potentially significant outcomes of their study have therefore been incorporated (Mechanisms 3a and 3b). The schematic in Fig. 6 summarises the major changes which have been made to the base mechanism, to allow a full appraisal of the impact of the RO₂ isomerisation chemistry, based on the parameters reported by Peeters et al. (2009). These include a number of important features, which are now summarised:

(i) a rigorous representation of the cis- and trans- isomers of the δ-hydroxyalkenyl peroxy radicals, to reflect that only the cis- isomers can potentially undergo isomerisations analogous to Reaction (R20);

(ii) a rigorous representation of the reversibility of O₂ addition to the “allyl-type” OH-isoprene adducts, which was calculated to be significant by Peeters et al. (2009). This allows redistribution of subsets of the peroxy radical population between the various isomers under atmospheric conditions, i.e., when their lifetimes with respect to onward reaction (with NO, HO₂ and RO₂) are comparable with, or longer than, those with respect to back decomposition;

(iii) inclusion of 1,6 H atom shift isomerisation reactions for each of the (newly-defined) cis- isomers of the δ-hydroxyalkenyl peroxy radicals, CISOPAO2 and CISOPCO2, at respective rates of 1 s⁻¹ and 8 s⁻¹ (based on the reported lower limits); followed by reaction with O₂ to yield HO₂ and a hydroperoxyaldehyde product. Peeters et al. (2009) thus calculate that these reactions are likely to be the dominant onward fates of these radicals, even at ppb levels of NO;

(iv) inclusion of 1,5 H atom shift isomerisation reactions for the β-hydroxyalkenyl peroxy radicals, ISOPBO2 and ISOPDO2 at respective rates of 4 × 10⁻³ s⁻¹ and 1.1 × 10⁻² s⁻¹ (based on the reported lower limits); followed by a concerted decomposition to yield OH, HCHO and either MVK or MACR. Peeters et al. (2009) thus calculate that these reactions provide a partial competition to Reactions (R10) and (R11) for these radicals at low NO_x.

With the exception of the hydroperoxyaldehyde products HPC41CHO (4-hydroperoxy-2-methyl-cis-but-2-enal) and HPC42CHO (4-hydroperoxy-3-methyl-cis-but-2-enal), no new first generation products are generated from the above mechanistic changes. The further degradation of these compounds was defined using the MCM protocol (Jenkin et al., 1997; Saunders et al., 2003), but without imposing the simplifications usually applied to species possessing hydroperoxide groups. The main features of the chemistry are

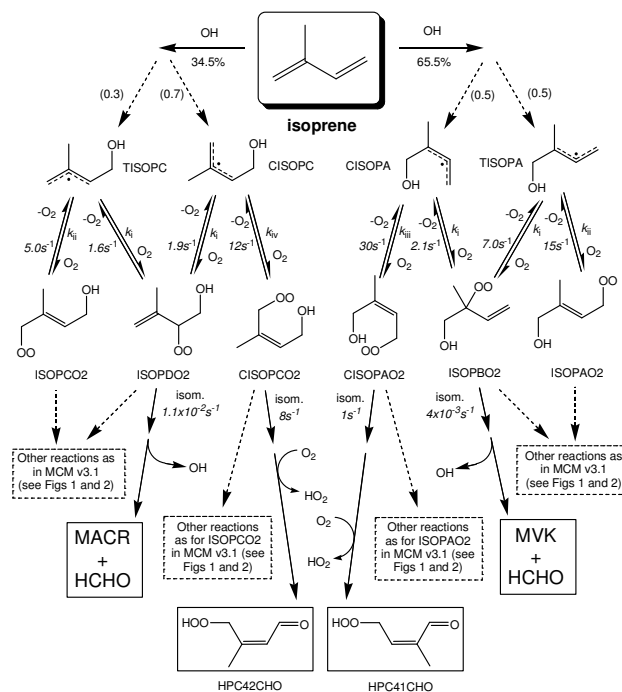


Fig. 6. Schematic representation of the OH initiated degradation of isoprene to first generation products in Mechanisms 3a and 3b. With the exception of the initial OH addition ratio, the mechanism and parameters are taken from the theoretical study of Peeters et al. (2009), and facilitate a full appraisal of the impact of the RO₂ isomerisation chemistry on HO_x recycling. $k_i = 1.5 \times 10^{-12}$ cm³ molecule⁻¹ s⁻¹; $k_{ii} = 3.0 \times 10^{-13}$ cm³ molecule⁻¹ s⁻¹; $k_{iii} = 1.4 \times 10^{-12}$ cm³ molecule⁻¹ s⁻¹; $k_{iv} = 1.0 \times 10^{-12}$ cm³ molecule⁻¹ s⁻¹. The initial OH addition ratio is unchanged from MCM v3.1 (see Sect. 2 and Fig. 1), but is very close to that calculated by Peeters et al. (2009).

shown schematically in Fig. 7 for HPC42CHO, with analogous pathways implemented for HPC41CHO. The complete updated chemistry in Mechanisms 3a and 3b resulted in an overall increase of 35 species and 132 reactions relative to the base case mechanism.

The further degradation of HPC41CHO and HPC42CHO in the initial update (Mechanism 3a) is dominated by removal initiated by reaction with OH. Although removal by photolysis is also represented, this makes only a minor contribution, based on the generic parameters applied to the photolysis of the hydroperoxide and α, β-unsaturated aldehyde (methacrolein-like) groups, which assume the chromophores are independent. However, Peeters et al. (2009) also pointed out that the combination of the relatively strongly-absorbing unsaturated aldehyde chromophore, and the weak O-O bond in the hydroperoxide group, provides the possibility of photolysis with a unity quantum yield, i.e., some two orders of magnitude greater than reported for methacrolein (e.g., Raber and Moortgat, 1996; Gierczac et al., 1997; Pinho et al., 2005), leading to the formation of OH as follows:

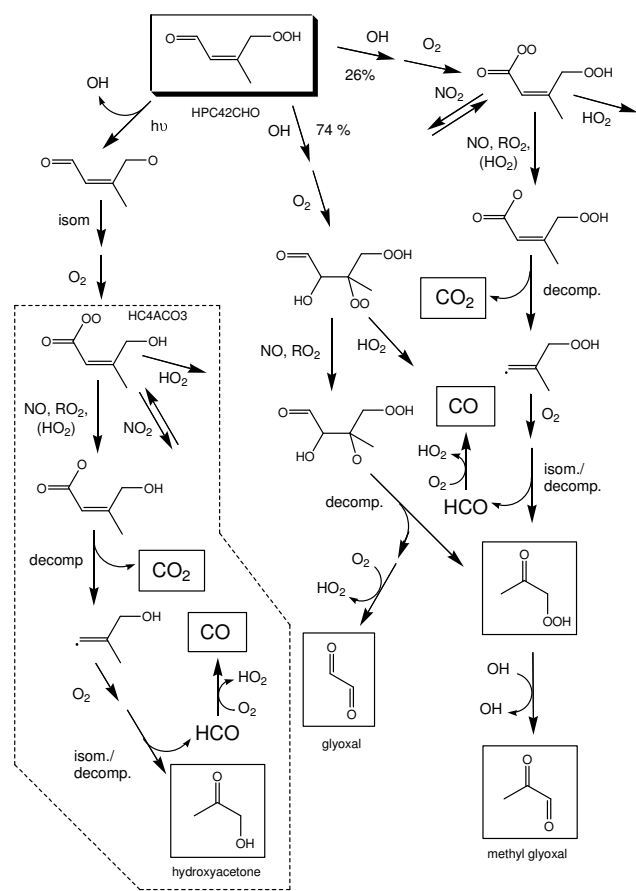
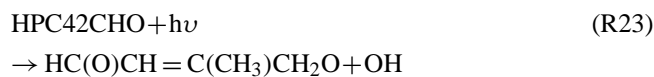
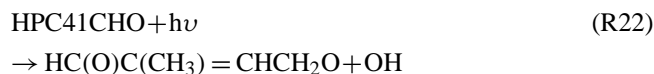


Fig. 7. Schematic representation of the degradation of the HPC42CHO as initiated by reaction with OH in Mechanisms 3a–3d, and as initiated by photolysis in Mechanisms 3b–3d (see text). The boxed chemistry is unchanged from MCM v3.1, although it is noted that Peeters et al. (2009) suggest additional HO_x formation may occur following isomerisation of HC4ACO3. For clarity, only the main propagating routes are shown, but competing reactions for peroxy radicals were fully represented in the mechanisms. Propagating channels for the reactions of HO₂ with the acyl peroxy radicals in this mechanistic extension were only represented in the consolidated Mechanism 4.



The impact of representing these reactions with appropriately elevated photolysis rates (daylight average $J_{22} = J_{23} \approx 5 \times 10^{-4} \text{ s}^{-1}$) was therefore also considered (Mechanism 3b). Photolysis at this rate would generally represent the dominant loss process for the hydroperoxy-methyl-butenal isomers.

The impact of using Mechanisms 3a and 3b, relative to the base MCM v3.1 (Mechanism 0) is shown in Figs. 3 and 4. Implementation of the isomerisation reactions without an elevated photolysis rate for HPC41CHO and HPC42CHO (Mechanism 3a) has a notable impact on the levels of OH, HO₂ and RO₂, with the effect becoming progressively larger as the NO_x level decreases. The respective mixing ratios of OH and HO₂ were simulated to increase by about 13% and 50% at the low end of the NO_x range, with that of RO₂ simulated to decrease by about 40% (see Fig. 4). The changes for HO₂ and RO₂ mainly reflect the enhanced conversion of the latter to the former via the 1,6 H-shift isomerisation chemistry for the cis- δ -hydroxyalkenyl peroxy radicals, whereas the increase in OH is mainly a result of its direct formation from the implementation of the 1,5 H atom shift isomerisation reactions for the β -hydroxyalkenyl peroxy radicals. Another feature, apparent in Fig. 3, is that the implementation of the chemistry in Mechanism 3a leads to slight increases in the simulated mixing ratios of NO_x for the given NO_x input rates towards the low end of the range. The NO_x increases are mainly due to a further reduced ability of the newly implemented chemistry to form oxidised organic nitrogen species (in particular isoprene nitrates via Reaction R7b), owing to the direct competition of the RO₂ isomerisation reactions as implemented in Mechanism 3a. Indeed, reductions in first-generation isoprene nitrate formation were simulated across the entire NO_x range, with these reductions ranging from about a factor of 2 towards the high end of the considered NO_x range, to about a factor of 6 at the low end of the range. It is noted that phenomenological reductions of this type could potentially help to reconcile laboratory determinations of isoprene nitrate yields, which are typically reported to be about 7–12% (see discussion in Sect. 2) with the lower values of about 4%, which have been obtained through optimising this aspect of a conventional mechanism on the basis of field observations (e.g., Horowitz et al., 2007), although it is recognised that such conclusions are also influenced by assumptions regarding the fate and lifetime of the nitrates (Perring et al., 2009).

As shown in Figs. 3 and 4, implementation of the enhanced photolysis of HPC41CHO and HPC42CHO via Reaction (R22), in conjunction with their formation via the 1,6 H-shift isomerisation reactions of the cis- δ -hydroxyalkenyl peroxy radicals (Mechanism 3b), leads to a much increased impact on HO_x radical levels, in particular on those of OH. The impact on both OH and HO₂ mixing ratios progressively increases with decreasing NO_x, up to respective increases of about 230% and 65% at the low end of the NO_x range, relative to Mechanism 0 (see Fig. 4). This result further illustrates that mechanistic changes which are required to yield the enhancements in OH levels which approach those which have been inferred from field observations require not only recycling of HO_x, but also significant net formation of OH via processes which are effectively chain branching; in this case through the combination of the

propagating isomerisation reactions with the radical-forming photolysis Reactions (R22) and (R23). This essentially allows values of $n > 1$ in the parameterisations of Butler et al. (2008) and Kubistin et al. (2008) to be achieved via an explicit mechanism. The increases in OH concentration of up to about 200% are also in good quantitative agreement with those inferred by Lelieveld et al. (2008) as required to close the model-measurement discrepancy gap, using the traceable MIM2 mechanism.

Although these results demonstrate that the Peeters et al. (2009) mechanism has obvious potential for addressing the atmospheric OH recycling issue, experimental verification of the mechanism framework and parameters is required. As indicated above, some indirect experimental support for the 1,6 H-shift isomerisation reactions of the *cis*- δ -hydroxyalkenyl peroxy radicals comes from the reported observation of the analogous process for δ -hydroxy peroxy radicals formed during alkane oxidation (Perrin et al., 1998; Jorand et al., 2003). In addition to this, evidence for the formation of the hydroperoxy-methyl-butenal isomers (HPC41CHO and HPC42CHO) in low yield (<10%) has recently been reported by Paulot et al. (2009a), during blacklight photolysis of H₂O₂/isoprene/air mixtures in the Caltech environmental chamber. The slow-photolysis conditions of their studies yielded relatively low concentrations of radicals (compared with many previous product studies), apparently allowing the unimolecular peroxy radical isomerisation reactions to compete to some extent with the expected dominant reactions with HO₂. Scoping simulations were therefore carried out to investigate the extent to which the Peeters et al. (2009) mechanism can be reconciled with the observations of Paulot et al. (2009a). As shown in Fig. 8, a reference simulation using Mechanism 2b (as described in the previous section) allows a good description of the observations reported by Paulot et al. (2009a), but with a slight overestimation of the mixing ratios of the isoprene-derived hydroperoxides and the subsequently-formed epoxydiols. Implementation of the RO₂ isomerisation reaction framework according to Peeters et al. (2009), using Mechanism 3a, confirms that RO₂ isomerisations are predicted to be competitive at the assigned rates, and results in major formation of the hydroperoxy-methyl-butenals (HPC41CHO and HPC42CHO) and suppression of hydroperoxide and epoxydiol mixing ratios to slightly below the observations of Paulot et al. (2009a). The simulated formation of the hydroperoxy-methyl-butenals using Mechanism 3a is clearly much greater than the <10% yield reported by Paulot et al. (2009a). However, additional implementation of their rapid photolysis in Mechanism 3b (as postulated by Peeters et al., 2009) results in substantial suppression of their collective mixing ratio, such that they are only predicted to be present at comparable levels to the hydroperoxides in the early stages of the experiment (see Fig. 8). Noting that the Mechanism 3b simulation results in a similar suppression of the hydroperoxide and epoxydiol mixing ratios to Mechanism 3a, a fur-

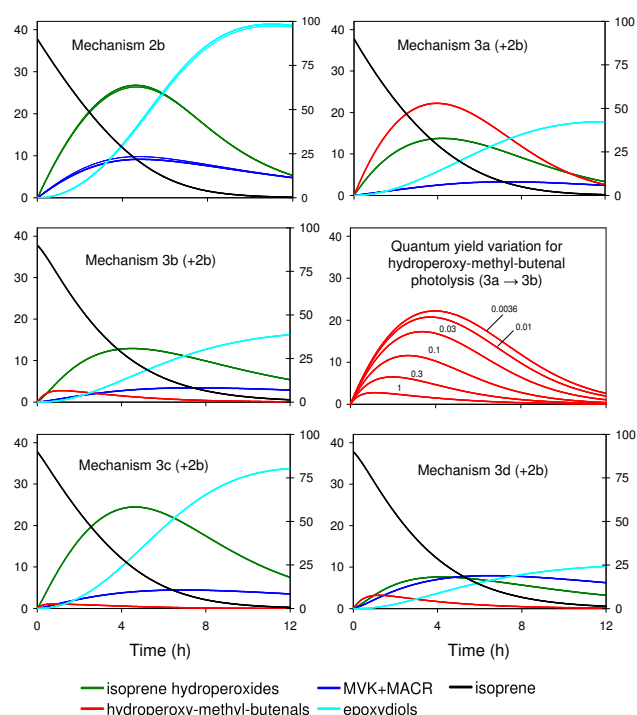


Fig. 8. Mechanism 3 scoping simulations for conditions representative of the H₂O₂-isoprene-air blacklight photolysis experiment reported in Fig. 1 of Paulot et al. (2009a), using Mechanism 2b as a reference (and with the associated epoxydiol formation also included in the Mechanism 3 variants). Isoprene mixing ratios (ppb) on right-hand axes; other species (ppb) on left-hand axes. Thin lines in Mechanism 2b panel show the influence of replacing parameterised RO₂ permutation reactions by an explicit representation, based on Jenkin et al. (1998). Initial conditions: 1.66 ppm H₂O₂ and 90 ppb isoprene. Calculations assumed a representative blacklight spectrum emitting over the range 330–400 nm ($\lambda_{\text{max}} \approx 355$ nm). Intensity scaled to achieve a factor of 3 reduction in isoprene mixing ratio after 4 hours. Absorption cross sections and quantum yields for H₂O₂ taken from Atkinson et al. (2004); absorption cross sections for methacrolein taken from Atkinson et al. (2006), with a quantum yield of 0.0036, as optimised by Pinho et al. (2005). Parameters for the hydroperoxy-methyl-butenals (HPC41CHO and HPC42CHO) based on methacrolein in Mechanism 3a, and on the methacrolein absorption cross sections in conjunction with a unity quantum yield in Mechanisms 3b, 3c and 3d. The effect of intermediate quantum yields on the simulated hydroperoxy-methyl-butenal profile is also shown for the transition from Mechanism 3a to 3b. Observed hydroperoxide mixing ratio after 3 h photolysis ≈ 18 ppb (Paulot et al., 2009a). Respective simulated hydroperoxide mixing ratios after 3 h photolysis are 23, 13, 12, 22 and 7 ppb with Mechanisms 2b, 3a, 3b, 3c and 3d.

ther simulation was carried out in which the rates of the isomerisation reactions for the *cis*- δ -hydroxyalkenyl and β -hydroxyalkenyl peroxy radicals were all decreased by an order of magnitude (denoted Mechanism 3c). In this respect, it is noted that da Silva et al. (2010) have recently reported 1,5

H atom shift isomerisation rates for the isoprene-derived β -hydroxyalkenyl peroxy radicals, calculated using DFT methods, which are about an order of magnitude lower than those reported by Peeters et al. (2009); although the isomerisation reactions of the δ -hydroxyalkenyl peroxy isomers were not considered in their study. As shown in Fig. 8, a simulation using the reduced rates in Mechanism 3c logically results in further suppression of the hydroperoxy-methyl-butenals, and an increase in the formation of the hydroperoxides and epoxydiols back to a similar level as simulated with Mechanism 2b. It appears, therefore, that the hydroperoxy-methyl-butenal observations reported by Paulot et al. (2009a) can probably support the operation of the Peeters et al. (2009) mechanism with these reduced RO₂ isomerisation rates, and that rates intermediate to those applied in Mechanism 3b and 3c would possibly provide the best simulation of hydroperoxide and epoxydiol formation.

As shown in Figs. 3 and 4, Mechanism 3c was also used to simulate the range of atmospheric reference scenarios. The order of magnitude reduction in the RO₂ isomerisation rates logically reduces the enhancement in simulated radical levels compared with Mechanism 3b, although the effect of the added chemistry is still notable. The impact on both OH and HO₂ mixing ratios once again progressively increases with decreasing NO_x, up to respective increases of about 100% and 30% at the low end of the NO_x range, relative to Mechanism 0 (see Fig. 4).

The mechanistic changes considered here also potentially have an impact on the simulated levels and distribution of well-established products of isoprene oxidation, for which characteristic ranges for atmospheric ratios are reasonably well-defined. Fig. 9 illustrates the impacts of the mechanistic changes on selected species ratios, namely MVK/MACR, glyoxal/methyl glyoxal, and the ratio of peroxy acetyl nitrate to peroxy methacrolyl nitrate, PAN/MPAN. In isoprene-dominated environments, these ratios have typically been reported to lie in the approximate ranges 0.8–2 for MVK/MACR (e.g., Spaulding et al., 2003; Kuhn et al., 2007; Karl et al., 2009), 4–10 for PAN/MPAN (e.g., Williams et al., 1997; Roberts et al., 2002, 2007), and 0.2–0.7 for glyoxal/methyl glyoxal (e.g., Lee et al., 1995, 1998; Spaulding et al., 2003). As shown in Fig. 9, Mechanisms 0 and 1, and the Mechanism 2 variants, generate ratios which are generally consistent with the reported ranges. However, implementation of the peroxy radical isomerisation chemistry postulated by Peeters et al. (2009) in Mechanisms 3a and 3b tends to increase the MVK/MACR ratios and PAN/MPAN ratios to uncharacteristic values, particularly towards the high end of the considered NO_x range. This observation is in agreement with the appraisal of Karl et al. (2009), who have previously demonstrated the impact of the Peeters et al. (2009) chemistry on MVK/MACR in relation to their observations at NO levels of about 100–300 ppt in the AMAZE campaign (which correspond to a daylight average NO_x level of about 2 ppb in our calculations). As also discussed in de-

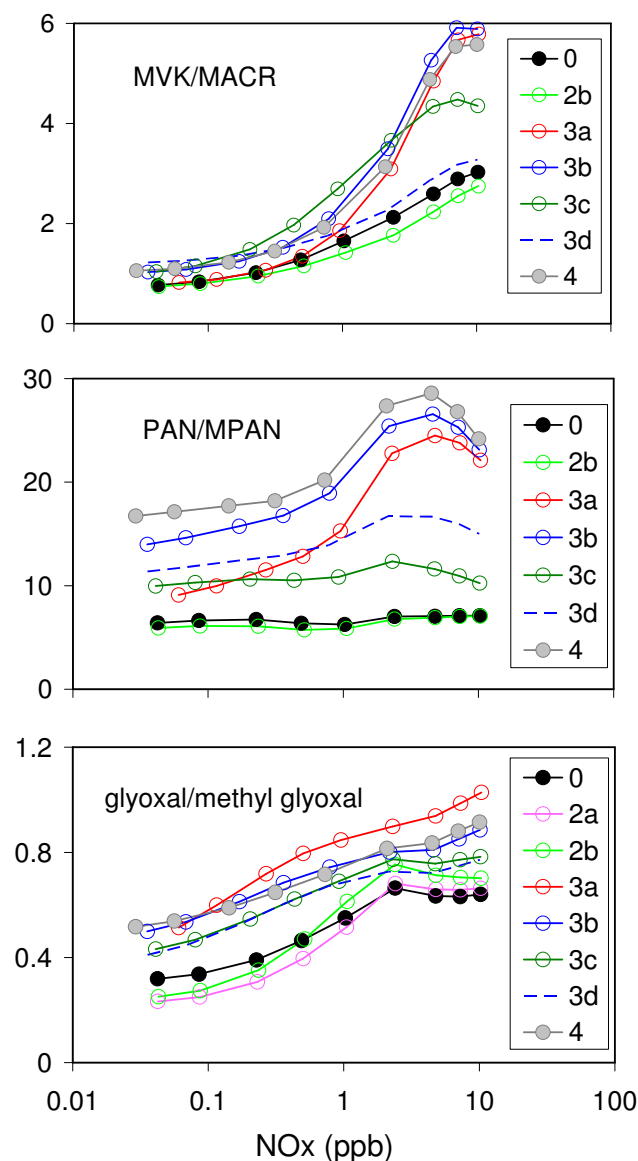


Fig. 9. Simulated product ratios for selected products of isoprene oxidation as a function of NO_x mixing ratio, using MCM v3.1 (Mechanism 0) and the mechanism variants described in Table 1. All values are daytime averages over the second day of the simulations, calculated from 06:00 to 18:00 local time in the model. Results for Mechanism 1 and Mechanism 2a (where not shown) are indistinguishable from Mechanism 0.

tail by Karl et al. (2009), the simulated product ratios are potentially sensitive to variation of many of the parameters within the mechanism postulated by Peeters et al. (2009), emphasising that there is potentially scope for reconciling the reaction framework with observational discrepancies through parameter refinement and optimisation.

This has been considered very recently by Peeters and co-workers (Stavrakou et al., 2010), who have suggested

the use of RO₂ isomerisation rate coefficients based on the geometric means of those reported previously by Peeters et al. (2009) for the pairs of *cis*- δ -hydroxyalkenyl and β -hydroxyalkenyl peroxy radicals, to address the MVK/MACR over-simulation issue. Specifically, they recommended applying a geometric mean of the previous rate coefficients (i.e. about 3 s⁻¹) for each of the *cis*- δ -hydroxyalkenyl peroxy radicals (CISOPAO2 and CISOPCO2), and five times the geometric mean of the previous rate coefficients (i.e. about 0.3 s⁻¹) for each of the β -hydroxyalkenyl peroxy radicals (ISOPBO2 and ISOPDO2). These adjustments were therefore also considered in the present work (denoted Mechanism 3d), with the changes being made as a refinement to Mechanism 3b (i.e. with rapid hydroperoxy-methyl-butenal photolysis maintained). As shown in Fig. 9, the changes do have the effect of reducing MVK/MACR at the high end of the NO_x range to values that are more comparable with the Mechanism 0 simulation. They also result in a reduction in the simulated PAN/MPAN ratios towards the observed range, although the values are still elevated (see Fig. 9). Although the formation of MACR relative to MVK is more consistent with observations as a result of the parameter changes in Mechanism 3d, the general suppression in the collective formation of MACR and MVK resulting from the operation of the competing δ -hydroxyalkenyl RO₂ isomerisation reactions remains, and this leads to a residual inhibition of MPAN formation compared with the base Mechanism 0. Noting that the use of generally reduced isomerisation rates in Mechanism 3c also logically has a lowering effect on the PAN/MPAN ratio (see Fig. 9), it is probable that the use of isomerisation rate coefficients based on the geometric means, in conjunction with a general reduction in their rates, can be reconciled with the range of atmospheric observations.

As shown in Figs. 3 and 4, the implementation of the parameter adjustments in Mechanism 3d leads to comparable impacts on the HO_x radical levels as Mechanism 3b, but with some additional increase resulting primarily from the scaling up of the isomerisation rates for the β -hydroxyalkenyl RO₂ radicals. This leads to maximum enhancements in OH and HO₂ of about 260% and 70% at the low end of the NO_x range, relative to Mechanism 0 (see Fig. 4). It is noted, however, that the additional increase in the β -hydroxyalkenyl RO₂ isomerisation rates recommended by Stavrakou et al. (2010) further worsens the agreement with the values calculated recently by da Silva et al. (2010), as commented on above. Stavrakou et al. (2010) justify the increase in terms of it being an optimisation to the yields of MVK and MACR reported in the chamber study of Paulot et al. (2009a), which were attributed to formation from the same isomerisation reactions. However, it is noted that the present simulations of the Paulot et al. (2009a) experiments (Fig. 8) are consistent with substantial formation of MVK and MACR resulting from the peroxy radical permutation reactions (e.g., via reaction sequence R8 and R10a), with these being the only sources of MVK and MACR in the Mecha-

nism 2b simulation. Their importance was also confirmed by replacing the MCM parameterised representation of the peroxy radical permutation reactions by the explicit chemistry reported in the kinetics study of Jenkin et al. (1998), which gave an almost identical result (see Fig. 8, Mechanism 2b panel). As also shown in Fig. 8, implementation of the Stavrakou et al. (2010) refinements in Mechanism 3d tends to increase MVK and MACR formation at the expense of hydroperoxide formation, and apparently worsens the agreement with the observations of Paulot et al. (2009a). In view of this, it appears that the elevation of the β -hydroxyalkenyl RO₂ isomerisation rate coefficients to the extent suggested by Stavrakou et al. (2010) cannot be fully justified on the basis of the Paulot et al. (2009a) data.

Finally, it is noted that the formation and rapid photolysis of the hydroperoxy-methyl-butenal isomers (HPC41CHO and HPC42CHO) predicted by the Peeters et al. (2009) mechanism provides routes to comparatively prompt formation of second-generation products of isoprene oxidation, on a timescale of about 30 min. As shown in Fig. 7, this potentially leads to the rapid generation of products such as hydroxyacetone (from HPC42CHO) and glycolaldehyde (from HPC41CHO), which are traditionally considered to be delayed products of isoprene oxidation. It is noted that such routes could help to address model measurement discrepancies in some studies, such as the underprediction of prompt hydroxyacetone formation reported for the AMAZE campaign by Karl et al. (2009). However, it is also noted that Dibble (2004a, b) has proposed routes to formation of glycolaldehyde and hydroxyacetone as minor first generation products, involving initial isomerisation of ISOPAO and ISOPCO, which could also help account for such observations.

The results presented here suggest that the chemical mechanism framework postulated by Peeters et al. (2009) provides a basis for representing substantial OH recycling/formation under tropospheric conditions, whilst also potentially helping to improve the simulation of certain other aspects of isoprene degradation chemistry in relation to reported field observations (i.e., suppression of first-generation isoprene nitrate formation and increased prompt production of hydroxyacetone). However, it is also clear that the mechanism with the reported parameters (as represented here by Mechanism 3b) cannot be fully reconciled with some other atmospheric observations (e.g., the characteristic ranges observed for the ratios MVK/MACR and PAN/MPAN), or with existing laboratory data (e.g., the chamber results of Paulot et al., 2009a) without some degree of parameter refinement and optimisation. The sensitivity tests presented above suggest that this would probably require some reduction and level of equalisation in the rate coefficients applied to the 1,6 H atom shift isomerisation reactions of the *cis*- δ -hydroxyalkenyl peroxy radicals, which would be accompanied by a decreased (but still significant) impact on HO_x levels. In view of this, it is clearly desirable that all aspects of the mechanism framework postulated by

Peeters et al. (2009) are evaluated by appropriately designed laboratory studies (i.e., under conditions of low NO_x and low RO₂ and HO₂ concentrations which have generally not been fully accessed in previous studies), including confirmation of the rapid photolysis of the hydroperoxy-methyl-butanal products, and the resultant formation of OH.

3.5 Combined impact of major changes

A further set of runs was carried out with a mechanism in which the major mechanistic changes described above in Mechanisms 1, 2b and 3b were combined (Mechanism 4). The aim here was to assess the maximum possible enhancement in HO_x levels which would result from the proposed mechanistic changes and to see if the effects are multiplicative. This procedure included the incorporation of radical propagating channels for the reactions of HO₂ with all newly-defined acyl peroxy and β-oxo peroxy radicals generated in Mechanisms 2b and 3b. The combined updated chemistry in Mechanism 4 resulted in an overall increase of 56 species and 200 reactions relative to the base case mechanism.

The impact of using Mechanism 4, relative to the base MCM v3.1 (Mechanism 0) is shown in Figs. 3, 4 and 9. The simulated effect on species mixing ratios is logically dominated by the implementation of the RO₂ isomerisation chemistry and associated rapid photolysis of HPC41CHO and HPC42CHO in Mechanism 3b, leading to respective increases of about 290%, 120% and 40% simulated for OH, HO₂ and RO₂, relative to Mechanism 0, at the low end of the NO_x range (see Fig. 4). Although the combined influence of the changes on OH radical levels is approximately multiplicative across the NO_x range, the effect on HO₂ radical levels is more than multiplicative, with an additional enhancement factor increasing from about 1.1 at 1 ppb NO_x to about 1.35 at the low end of the NO_x range. This is interpreted in terms of the impact of the implementation of the radical propagating channels for the reactions of HO₂ with the newly-defined acyl peroxy RO₂ radicals generated in Mechanism 3b, and to a lesser extent the newly-defined β-oxo RO₂ radicals generated in Mechanism 2b. As shown in Figs. 5 and 7, these reactions for the specific multifunctional RO₂ radical structures formed tend to lead to prompt generation of HO₂ from the RO product (rather than formation of a further RO₂ radical, as in the case of CH₃C(O)O₂ for example) such that the reaction channels are HO₂-neutral.

Although the mechanistic changes implemented here allow substantial increases in OH recycling and formation, it is noted that the simulated HO₂/OH ratios towards the low end of the NO_x range with all the considered mechanistic variants are consistently greater than those observed. In the base case MCM v3.1 simulation (Mechanism 0), the level of overestimation (about a factor of 4–6) is comparable with that reported previously by Kubistin et al. (2008) using the same mechanism. With the exception of partial implementation of

the chemistry proposed by Peeters et al. (2009) (Mechanism 3a), the suite of mechanistic changes considered here all decrease the HO₂/OH ratio under almost all considered conditions because the enhancements in simulated OH concentration are greater than those for HO₂ (see Fig. 4), and therefore lead to some improvement in relation to the observed ratios. A number of studies have shown that simulations with a variety of atmospheric chemical mechanisms invariably tend to overestimate measured HO₂/OH ratios at low NO_x, compared with observations (e.g., Chen et al., 2009 and references therein), and it appears that the discrepancy is not specific to isoprene-dominated environments. It potentially has contributions from issues related to both measurements and chemical mechanisms, which clearly require further investigation. The former may include impacts related to data averaging of a non-linear ratio, if there are fluctuations in NO_x level (i.e., dynamical effects); and to imprecision in the measurement of the NO_x species (particularly NO), if measurements are close to instrumental detection limits. Chemical mechanism issues may relate to incomplete understanding and representation of the gas phase pathways, or to a general lack of representation of a loss process for HO₂ in all studies (e.g., aerosol uptake), which potentially becomes more important at low NO_x when the lifetime of HO₂ with respect to gas phase loss increases.

4 Global model studies

To facilitate investigation of the impact of the mechanistic changes represented in the combined Mechanism 4 in chemistry-transport models, a substantially reduced representation was developed for use with version 2 of the Common Representative Intermediates mechanism (CRI v2) and its reduced variants. As described by Jenkin et al. (2008b), CRI v2 is a lumped chemistry mechanism of intermediate complexity, the performance of which is traceable to MCM v3.1. The isoprene mechanism represents a substantial reduction over that in MCMv3.1, represented by 28 species and 95 reactions. It has recently been evaluated in the isoprene mechanism intercomparison of Archibald et al. (2009) and its performance was found to be in good agreement with that of MCM v3.1 over a wide range of conditions. The CRI v2 isoprene mechanism is also an unchanged component of a set of reduced, emissions-lumped CRI v2 variants (Watson et al., 2008), the most reduced of which (CRI v2-R5) has been very recently implemented into a global model (Utembe et al., 2010).

The changes outlined above for Mechanism 1 were readily incorporated into the CRI v2 chemistry, the intermediate RO₂ radicals possessing acyl or β-oxo character being easily identifiable. No change was made in relation to Mechanism 2b, because the set of isoprene-derived hydroperoxides is represented by a single lumped species (RU14OOH), the OH-initiated degradation of which already quantitatively

regenerates OH by a process analogous to that shown above in Reactions (R14)–(R16). This means that the OH enhancements associated with Mechanism 2b (i.e., up to about 16%, as reported above in Sect. 3.3) are already effectively implicit in CRI v2 and are therefore not reflected in the sensitivity tests described below. The most challenging adaptation relates to incorporation of the RO₂ radical isomerisations (Mechanisms 3b), because the complete set of isoprene-derived peroxy radicals is represented by the single lumped species, RU14O2 (as is the case for most reduced isoprene mechanisms). In CRI v2, conventional reactions of RU14O2 with NO, HO₂ and the peroxy radical pool are represented. Two additional reactions were added, to represent isomerisation of the β -hydroxyalkenyl RO₂ isomers (Reaction R24) and the $\text{cis-}\delta$ -hydroxyalkenyl RO₂ isomers (Reaction R25),



(here, UCARB10 is a lumped C₄ carbonyl product which represents both MVK and MACR in CRI v2, and HPUCARB12 is a newly-defined hydroperoxyaldehyde product which corresponds to HPC41CHO and HPC42CHO in the detailed mechanism). The competition of these reactions with the alternative reactions for RU14O2 was determined by running a set of reference box model simulations using the detailed mechanism illustrated in Fig. 6 and represented in Mechanism 3b. In these simulations, the NO concentration was fixed at a set of values over the range 2.46×10^7 – 2.46×10^{12} molecule cm⁻³ (1 ppt – 100 ppb at 298K and 760 Torr), and the combined formation rate of the products from each type of isomerisation reaction was quantified relative to the formation rate of products derived from the combined (pseudo-first order) reaction of all the RO₂ isomers with NO. The global first order loss rates for the RO₂ + NO reactions could then be used to define effective rate coefficients (k_{24} and k_{25}) for each type of RO₂ isomerisation reaction for the complete range of conditions. The derived values of k_{24} and k_{25} were found to vary with NO concentration because, as indicated above in Sect. 3.4, the relative population of the RO₂ isomers changes with NO_x level by virtue of the reversibility of O₂ addition. However, the variation was found to be modest at levels of NO less than about 10^{10} molecule cm⁻³ (i.e., when the isomerisation reactions are able to compete more significantly), such that low NO_x limiting values of $k_{24} = 4 \times 10^{-3}$ s⁻¹ and $k_{25} = 8 \times 10^{-2}$ s⁻¹ could reasonably be assigned, and this assumption was made in the work presented here. The procedure was also repeated using RO₂ isomerisation rates reduced by an order of magnitude (i.e., as considered in the detailed Mechanism 3c above). The resultant values of k_{24} and k_{25} were also reduced by an order of magnitude, demonstrating a linear relationship between the detailed and reduced representations over this isomerisation parameter range. It is noted that the generic rate coefficient assigned to the competing reactions of the RO₂

radicals with NO in both the detailed and reduced mechanisms, 8.5×10^{-12} cm³ molecule⁻¹ s⁻¹ (at 298 K), agrees well with the consensus of recently reported values for isoprene-derived peroxy radicals (e.g., Miller et al., 2004, and references therein; IUPAC, 2010).

The hydroperoxyaldehyde product, HPUCARB12, was degraded via both reaction with OH and photolysis to generate appropriate intermediates already represented in CRI v2, with the photolysis reaction generating OH as follows:



The co-product, RU12O2, is a lumped radical used to represent an appropriate set of species in MCM v3.1, which includes the species HC4ACO3 formed by the analogous process in the detailed mechanism (see Fig. 7). In the reduced mechanism, the photolysis rate was set to correspond to the high value applied in Mechanism 3b and in the full detailed mechanism, Mechanism 4.

The global impacts of inclusion of HO_x formation and recycling from isoprene oxidation were investigated using an updated version of the UK Meteorological Office tropospheric chemistry transport model (STOCHEM) originally described by Collins et al. (1997). STOCHEM is a global 3-dimensional CTM which uses a Lagrangian approach to advect 50 000 air parcels using a 4th-order Runge-Kutta scheme with advection time steps of 3 h. The transport and radiation models are driven by archived meteorological data, generated by using the UK Meteorological Office numerical weather prediction models as analysis fields, with a resolution of 1.25° longitude and 0.83° latitude and on 12 vertical levels extending to 100 hPa. Full details of the model version employed are given in Derwent et al. (2008), with recent updates (including implementation of the CRI v2-R5 chemistry) reported in detail by Utembe et al. (2010).

Two experiments were performed to investigate the impacts of the mechanistic revisions described above, and a base case reference run against which the results could be compared using the unmodified CRI v2-R5 chemistry (Utembe et al., 2010). In each run, the model was allowed to spin up for a period of 12 months, and analysis was performed on the subsequent 12 months of data. The first sensitivity experiment (denoted Mechanism 4R) involved use of the optimised reduced mechanism described above, which is representative of a consolidation of all the mechanistic changes and is expected to yield particularly notable impacts on simulated OH radical levels in remote areas characterised by high emission rates of isoprene. In view of the results of the sensitivity tests presented above in Sect. 3.4, the second experiment investigated the impact of reducing the efficiency of the dominant peroxy radical isomerisation chemistry derived from the study of Peeters et al. (2009). This was achieved through reducing the peroxy radical isomerisation rates, k_{24} and k_{25} , by an order of magnitude (denoted Mechanism 4Ra), to allow comparison with the impact of

Table 2. Mixing ratio and percentage changes from the base case for a selection of species in a 5°×5°×~1 km grid box centred at 2.5° S and 67.5° W representative of the Amazon Forest. % = ((Sensitivity Run-BASE)/BASE)·100.

Period	OH (ppt)	HO ₂ (ppt)	NO _x (ppt)	O ₃ (ppb)	isoprene (ppb)
Base					
February	0.018	11.5	497.4	43.4	6.4
August	0.022	8.8	519.6	45.9	4.1
Annual Mean	0.028	9.9	590.2	52	3.9
	OH (%)	HO ₂ (%)	NO _x (%)	O ₃ (%)	isoprene (%)
Mech. 4R					
February	39.0	30.0	-1.6	0.0	-26.7
August	37.8	35.3	-5.6	-3.4	-21.5
Annual Mean	29.7	28.7	-4.8	-3.0	-23.3
Mech. 4Ra					
February	14.6	11.7	-2.6	0.3	-8.8
August	15.1	13.0	-2.7	-0.9	-6.9
Annual Mean	12.9	11.0	-3.1	-0.7	-7.9

Table 3. Mixing ratio and percentage changes from the base case for a selection of species in a 5°×5°×~1 km grid box centred at 2.5° N and 117.5° E representative of Borneo. % = ((Sensitivity Run-BASE)/BASE)·100.

Period	OH (ppt)	HO ₂ (ppt)	NO _x (ppt)	O ₃ (ppb)	isoprene (ppb)
Base					
February	0.049	7.9	204.7	21.9	1.1
August	0.066	8.0	349.0	25.5	0.6
Annual Mean	0.059	8.5	319.5	26.7	1.0
	OH (%)	HO ₂ (%)	NO _x (%)	O ₃ (%)	isoprene (%)
Mech. 4R					
February	24.6	34.0	2.9	-4.6	-29.2
August	22.5	31.6	-5.0	-4.6	-21.1
Annual Mean	23.2	30.9	-1.4	-4.9	-25.4
Mech. 4Ra					
February	11.1	15.5	0.2	-1.8	-14.6
August	9.7	12.3	-2.7	-1.6	-9.1
Annual Mean	9.9	12.6	-1.6	-1.8	-11.5

the similar sensitivity test performed with the detailed mechanism (i.e., Mechanism 3c vs. Mechanism 3b) as described in Sect. 3.4. The results of these experiments are summarised in Fig. 10, and in Tables 2 and 3.

The effect on the simulated monthly-mean OH concentrations in the surface model layer relative to the base case is shown in Fig. 10, for the example months of February and August. Increases in OH levels are generally simulated for all land areas with Mechanism 4R (panels a and b), whilst changes over the oceans tend to be close to zero. Logically, the greatest increases (up to about 40%) are simulated for regions where isoprene emissions are highest and NO_x emissions are lowest (the tropics in February and the tropics as well as forested boreal regions in August). The general pattern is therefore similar to that reported by Lelieveld et

al. (2008) and Butler et al. (2008), using parameterised representations of OH recycling based on optimisation to observations, and also to that reported recently by Stavrou et al. (2010) using a reduced explicit representation of an adjusted version of the Peeters et al. (2009) mechanism.

Tables 2 and 3 summarise the results for selected species for the 5°×5°×~1 km surface grid boxes representative of the tropical forests of the Amazon (centred on 2.5° S, 67.5° W) and Borneo (centred on 2.5° N, 117.5° E), which are broadly relevant to the locations of the recently reported HO_x measurements (Lelieveld et al., 2008; Pugh et al., 2010a). The simulated enhancements in OH over the Amazon with Mechanism 4R (Table 2) are about 40% in both February and August, with a concurrent reduction of approximately 25% in isoprene mixing ratios. Although these

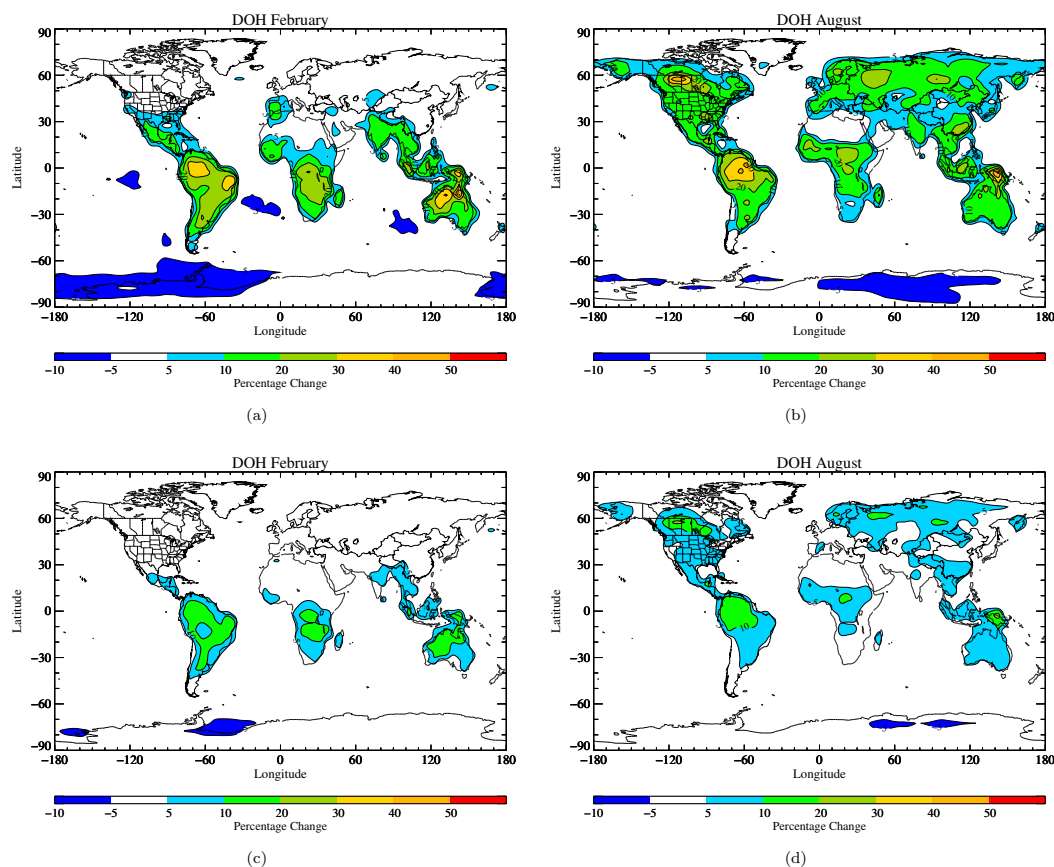


Fig. 10. Percentage difference plots for the global model sensitivity runs, relative to the base case for OH. $\% = ((\text{Run}-\text{Base})/\text{Base}) \cdot 100$: (a) February, Mechanism 4R; (b) August, Mechanism 4R; (c) February, Mechanism 4Ra; (d) August, Mechanism 4Ra.

changes are somewhat smaller than those simulated at the low end of the NO_x range in the box model studies, it should be noted that the global model resolution is fairly coarse, such that regions of particularly low NO_x cannot be adequately resolved. As a result, the simulated NO_x mixing ratios (about 500 ppt) are much greater than those reported for the specific pristine forest locations, which are typically 20–50 ppt (Lelieveld et al., 2008; Butler et al. 2008). However, the changes in OH mixing ratios are fully consistent with those calculated for comparable conditions in the box modelling studies (e.g., the box model simulation with Mechanism 4 predicts respective changes in daytime-averaged OH and isoprene levels of 53% and –31% relative to the Mechanism 0 base case run which yielded a daytime-averaged NO_x level of 489 ppt and an isoprene level of 6.1 ppb). This suggests that a calculation at finer resolution could yield the enhancements in OH levels of about 200% predicted in the box model studies at the low end of the considered NO_x range (about 40 ppt), and as also calculated by Lelieveld et al. (2008) using a higher resolution model with a parameterised representation of OH recycling. It is also noted that Stavrakou et al. (2010) have recently reported similar en-

hancements using a reduced explicit representation derived from the Peeters et al. (2009) mechanism. The changes in OH levels (23–25%) simulated for the Borneo grid box with Mechanism 4R (Table 3) are slightly smaller than those for the Amazon, even though the simulated NO_x mixing ratios are lower (about 200–300 ppt). This reflects a compensating influence of the generally lower modelled abundance of isoprene in this region, which leads to a partial dilution in the impact of the chemistry. As shown in Tables 2 and 3 the mechanistic changes implemented in Mechanism 4R lead to increases of about 30% in HO₂ radical levels which is also consistent with the results of the box model studies.

An order of magnitude reduction in the rates of the peroxy radical isomerisation reactions, k_{24} and k_{25} (Mechanism 4Ra), leads to a reduced but still notable impact. The geographical changes in OH levels (Fig. 10, panels c and d) show the same general pattern as those simulated with Mechanism 4R, with maximum increases of about 15% relative to the base case. The effects on all the species for the example Amazon and Borneo locations (Tables 2 and 3) are consistently just over a factor of two lower than those simulated with Mechanism 4R, a sensitivity which is fully consistent

with that observed in the detailed box modelling studies. This suggests that a calculation at fine resolution with Mechanism 4Ra could result in enhancements in OH levels of approximately 100%, as predicted in the box model studies at the low end of the considered NO_x range.

It is interesting to note that, although the dominant regional impact on OH formation results from the isoprene-specific chemistry involving the peroxy radical isomerisation reactions, the implementation of the propagating channels for the reactions of HO₂ with relevant RO₂ radicals (particularly CH₃C(O)O₂) has a comparable globally-integrated impact. This is because the chemistry is relevant not only to the degradation of isoprene, but also to the degradation of the majority of emitted anthropogenic and biogenic VOCs.

5 Summary and conclusions

The sensitivity of isoprene degradation chemistry to a number of detailed mechanistic changes has been examined using MCM v3.1 as a reference base case mechanism, with particular focus on the impacts of these changes on the recycling and formation of OH radicals. Implementation of radical propagating channels for the reactions of HO₂ with relevant classes of organic peroxy radical (namely acyl and β-oxo peroxy radicals) resulted in a comparatively small impact on the system, leading to increases of about 5–7% in the concentrations of OH over the sub-ppb NO_x range. Implementation of the OH-catalysed conversion of the isoprene-derived hydroperoxides to isomeric epoxydiols, and representation of their subsequent degradation (based on the study of Paulot et al., 2009a), resulted in OH increases of up to about 16% relative to MCM v3.1, and potentially as high as about 25% if the chemistry replaces a representation of hydroperoxide chemistry with zero OH regeneration. However, it is noted that implementation of the Paulot et al. (2009a) chemistry has a near-zero effect on simulated OH if the existing representation of hydroperoxide chemistry is already fully OH-neutral, as is the case in some mechanisms (e.g., CRI v2).

Much greater potential impacts were achieved by implementation of a recently postulated mechanism involving isomerisation of the cis-δ-hydroxyalkenyl and β-hydroxyalkenyl peroxy radical isomers, formed from the sequential addition of OH and O₂ to isoprene, and rapid photolysis of the hydroperoxy-methyl-butenal products formed following the cis-δ-hydroxyalkenyl peroxy radical isomerisations (Peeters et al., 2009). This mechanism yielded a factor of up to 3.3 increase in the simulated OH concentration, maximising at the low end of the considered NO_x range, and possesses some features which could help improve selected aspects of model-measurement comparisons (e.g., suppression of isoprene nitrate formation and a relatively prompt formation route for hydroxyacetone). However, the results of additional sensitivity tests suggest that the mechanism with the reported parameters cannot be fully reconciled with

certain other atmospheric observations and existing laboratory data (such as the results of Paulot et al., 2009a) without some degree of parameter refinement and optimisation, which would probably require a reduction of, and some level of equalisation in, the isomerisation rates applied to the pair of cis-δ-hydroxyalkenyl peroxy radical isomers. An order of magnitude reduction in all the isomerisation rates was investigated, and was still found to yield notable enhancements in OH concentrations of up to a factor of about 2, indicating that the mechanism remains potentially significant even with this substantial parameter adjustment. It is important, therefore, that the details of the mechanism proposed by Peeters et al. (2009) are either confirmed or refuted by laboratory study, under conditions of low NO_x and low RO₂ and HO₂ concentrations, which have generally not been fully accessed in previous studies. It is noted that such studies would also facilitate a stringent evaluation of all isoprene mechanisms currently in use, for application under tropospheric conditions.

Application of a parameterized representation of the mechanistic changes in the STOCHEM global chemistry-transport model demonstrated that the greatest impact of the modified chemistry on OH concentrations logically occurs in remote regions characterized by high emission rates of isoprene, although a widespread low-level global impact also results from the processes which are not isoprene-specific (namely, implementation of the propagating channels of the reactions of HO₂ with relevant RO₂ radicals, particularly CH₃C(O)O₂). The magnitude of the impact in the high isoprene emission regions was found to be consistent with that observed in the box model sensitivity studies, with the results being illustrated and discussed with a particular focus on the tropical forested regions of the Amazon and Borneo, where unexpectedly elevated concentrations of OH have recently been reported.

Acknowledgements. The authors gratefully acknowledge support from: (a) GWR and the UK Meteorological Office for a studentship for ATA; (b) EPSRC for a studentship for MCC; (c) NERC as part of the APPRAISE ACES consortium (NE/E011217/1), and Defra (under contract AQ 0704) for MEJ; (d) NERC grant NE/D001846/1, forming part of the QUEST Deglaciation project, for SRU. The development of STOCHEM was supported by Defra through their SSNIP contract AQ 0902 (RGD). We are also grateful to the anonymous reviewers, and to Thomas Karl (NCAR) and Paul Wennberg (California Institute of Technology), for review comments and feedback which helped us to produce an improved manuscript.

Edited by: P. O. Wennberg

References

- Archibald, A. T., Jenkin, M. E., and Shallcross, D. E.: An isoprene mechanism intercomparison, *Atmos. Environ.*, doi:10.1016/j.atmosenv.2009.09.016, accepted, 2009.
- Atkinson, R., Baulch, D. L., Cox, R. A., Crowley, J. N., Hampson, R. F., Hynes, R. G., Jenkin, M. E., Rossi, M. J. and Troe J.: Evaluated kinetic and photochemical data for atmospheric chemistry: Volume I – gas phase reactions of O_x, HO_x, NO_x and SO_x species, *Atmos. Chem. Phys.*, 4, 1461–1738, doi:10.5194/acp-4-1461-2004, 2004.
- Atkinson, R., Baulch, D. L., Cox, R. A., Crowley, J. N., Hampson, R. F., Hynes, R. G., Jenkin, M. E., Rossi, M. J., and Troe J.: Evaluated kinetic and photochemical data for atmospheric chemistry: Volume II – reactions of organic species. *Atmos. Chem. Phys.*, 6, 3625–4055, doi:10.5194/acp-6-3625-2006, 2006.
- Baker, J., Arey, J., and Atkinson, R.: Formation and reaction of hydroxycarbonyls from the reaction of OH radicals with 1,3-butadiene and isoprene, *Environ. Sci. Technol.*, 39, 4091–4099, 2005.
- Benkelberg, H.-J., Böge, O., Seuwen, R., and Warneck, P.: Product distributions from the OH radical-induced oxidation of but-1-ene, methyl-substituted but-1-enes and isoprene in NO_x-free air, *Phys. Chem. Chem. Phys.*, 2, 4029–4039, 2000.
- Butler, T. M., Taraborrelli, D., Brühl, C., Fischer, H., Harder, H., Martinez, M., Williams, J., Lawrence, M. G., and Lelieveld, J.: Improved simulation of isoprene oxidation chemistry with the ECHAM 5/MESSy chemistry-climate model: lessons from the GABRIEL airborne field campaign, *Atmos. Chem. Phys.*, 8(16), 4529–4546, 2008.
- Calvert, J. G., Atkinson, R., Kerr, J. A., Madronich, S., Moortgat, G. K., Wallington, T. J., and Yarwood, G.: *The Mechanisms of Atmospheric Oxidation of Alkenes*, Oxford University Press, New York, USA, ISBN: 0195131770, 2000.
- Chen, S., Ren, X., Mao, J., Chen, Z., Brune, W. H., Lefer, B. Rappenglück, B., Flynn, J., Olson, J., and Crawford, J. H.: A comparison of chemical mechanisms based on TRAMP-2006 field data, *Atmos. Environ.*, doi:10.1016/j.atmosenv.2009.05.027, 2009.
- Collins, W., Stevenson, D., Johnson, C., and Derwent, R.: Tropospheric Ozone in a Global-Scale Three-Dimensional Lagrangian Model and Its Response to NO_x Emission Controls, *J. Atmos. Chem.*, 26(3), 223–274, 1997.
- Derwent, R. G., Stevenson, D. S., Doherty, R. M., Collins, W. J., Sanderson, M. G., and Johnson, C. E.: Radiative forcing from surface NO_x emissions: spatial and seasonal variations, *Clim. Change*, 88(4), 385–401, 2008.
- Da Silva, G., Graham, C., and Wang, Z.-F.: Unimolecular β -hydroxyperoxy radical decomposition with OH recycling in the photochemical oxidation of isoprene, *Environ. Sci. Technol.*, 44, 250–256, 2010.
- Dibble, T. S.: Intramolecular hydrogen bonding and double H-atom transfer in peroxy and alkoxy radicals from isoprene, *J. Phys. Chem. A.*, 108, 2199–2207, 2004a.
- Dibble, T. S.: Prompt chemistry of alkenoxy radical products of the double H-atom transfer of alkoxy radicals from isoprene, *J. Phys. Chem. A.*, 108, 2208–2215, 2004b.
- Dillon, T. J. and Crowley, J. N.: Direct detection of OH formation in the reactions of HO₂ with CH₃C(O)O₂ and other substituted peroxy radicals, *Atmos. Chem. Phys.*, 8(16), 4877–4889, doi:10.5194/acp-8-4877-2009, 2008.
- Dlugi, R., Berger, M., Zelger, M., Hofzumahaus, A., Siese, M., Holland, F., Wisthaler, A., Grabmer, W., Hansel, A., Koppmann, R., Kramm, G., Möllmann-Coers, M. and Knaps, A.: Turbulent exchange and segregation of HO_x radicals and volatile organic compounds above a deciduous forest, *Atmos. Chem. Phys.*, 10, 6215–6235, doi:10.5194/acp-10-6215-2010, 2010.
- Eerdekens, G., Ganzeveld, L., Vilà-Guerau de Arellano, J., Klüpfel, T., Sinha, V., Yassaa, N., Williams, J., Harder, H., Kubistin, D., Martinez, M., and Lelieveld, J.: Flux estimates of isoprene, methanol and acetone from airborne PTR-MS measurements over the tropical rainforest during the GABRIEL 2005 campaign, *Atmos. Chem. Phys.*, 9, 4207–4227, doi:10.5194/acp-9-4207-2009, 2009.
- Gierczak, T., Burkholder, J. B., Talukdar, R. K., Mellouki, A., Barone, S. B., and Ravishankara, A. R.: Atmospheric fate of methyl vinyl ketone and methacrolein, *J. Photochem. Photobiol. A: Chemistry*, 110, 1–10, 1997.
- Greenwald, E., North, S., Georgievskii, Y., and Klippenstein, S.: A two transition state model for radical-molecule reactions: applications to isomeric branching in the OH-isoprene reaction, *J. Phys. Chem. A.*, 111, 5582–5592, 2007.
- Guenther, A., Hewitt, C. N., Erickson, D., Fall, R., Geron, C., Graedel, T., Harley, P., Klinger, L., Lerdau, M., McKay, W.A., Pierce, T., Scholes, B., Steinbrecher, R., Tallamraju, R., Taylor, J., and Zimmerman, P.: A global model of natural volatile organic compound emissions, *J. Geophys. Res.*, 100, 8873–8892, 1995.
- Hasson, A. S., Tyndall, G. S. and Orlando, J. J.: A product yield study of the reaction of HO₂ Radicals with ethyl peroxy (C₂H₅O₂), acetyl peroxy (CH₃C(O)O₂), and acetonyl peroxy (CH₃C(O)CH₂O₂) radicals, *J. Phys. Chem. A.*, 108(28), 5979–5989, 2004.
- Heard, D. E. and Pilling, M. J.: Measurement of OH and HO₂ in the troposphere, *Chem. Rev.*, 103(12), 5163–5198, 2003.
- Horowitz, L. W., Fiore, G. P., Milly, A. M., Cohen, R. C., Perrin, A., Wooldridge, P. J., Hess, P. G., Emmons, L. K., and Lamarque, J.: Observational constraints on the chemistry of isoprene nitrates over the eastern United States, *J. Geophys. Res.*, 112(D12), D12S08, doi:10.1029/2006JD007747, 2007.
- IUPAC: Current recommendation of the IUPAC Subcommittee for Gas Kinetic Data Evaluation, available at: <http://www.iupac-kinetic.ch.cam.ac.uk/>, 2010.
- Jenkin, M. E. and Clemitshaw K. C.: Ozone and other secondary photochemical pollutants: chemical processes governing their formation in the planetary boundary layer, *Atmos. Environ.*, 34, 2499–2527, 2000.
- Jenkin, M. E., Saunders, S. M., and Pilling, M. J.: The tropospheric degradation of volatile organic compounds: a protocol for mechanism development, *Atmos. Environ.*, 31(1), 81–104, 1997.
- Jenkin, M. E., Boyd, A. A., and Lesclaux, R.: Peroxy radical kinetics resulting from the OH-initiated oxidation of 1, 3-butadiene, 2, 3-dimethyl-1, 3-butadiene and isoprene, *J. Atmos. Chem.*, 29(3), 267–298, 1998.
- Jenkin, M. E., Hurley, M. D., and Wallington, T. J.: Investigation of the radical product channel of the CH₃C(O)O₂ + HO₂ reaction in the gas phase, *Phys. Chem. Chem. Phys.*, 9(24), 3149–3162, 2007.
- Jenkin, M. E., Hurley, M. D., and Wallington, T. J.: Investigation of

- the radical product channel of the CH₃C(O)CH₂O₂ + HO₂ reaction in the gas phase, *Phys. Chem. Chem. Phys.*, 10(29), 4274–4280, 2008a.
- Jenkin, M. E., Watson, L. A., Utembe, S. R., and Shallcross, D. E.: A Common Representative Intermediates (CRI) mechanism for VOC degradation. Part 1: Gas phase mechanism development, *Atmos. Environ.*, 42(31), 7185–7195, 2008b.
- Jenkin, M. E., Hurley, M. D., and Wallington, T. J.: Investigation of the radical product channel of the CH₃OCH₂O₂ + HO₂ reaction in the gas phase, *J. Phys. Chem. A*, 114, 408–416, 2010.
- Jorand, F., Heiss, A., Perrin, O., Sahetchian, K., Kerhoas, L., and Einhorn, J.: Isomeric hexyl-ketohydroperoxides formed by reactions of hexoxy and hexylperoxy radicals in oxygen, *Int. J. Chem. Kinet.*, 35(8), 354–366, 2003.
- Karl, T., Guenther, A., Turnipseed, A., Tyndall, G., Artaxo, P. and Martin, S.: Rapid formation of isoprene photo-oxidation products observed in Amazonia, *Atmos. Chem. Phys.*, 9, 7753–7767, doi:10.5194/acp-9-7753-2009, 2009.
- Kubistin, D., Harder, H., Martinez, M., Rudolf, M., Sander, R., Bozem, H., Eerdeken, G., Fischer, H., Gurk, C., Klpfel, T., Knigstedt, R., Parchatka, U., Schiller, C. L., Stickler, A., Taraborrelli, D., Williams, J. and Lelieveld, J.: Hydroxyl radicals in the tropical troposphere over the Suriname rainforest: comparison of measurements with the box model MECCA, *Atmos. Chem. Phys. Discuss.*, 8(4), 15239–15289, doi:10.5194/acpd-8-15239-2008, 2008.
- Kuhn, U., Andreae, M. O., Ammann, C., Araújo, A. C., Brancaleoni, E., Ciccioli, P., Dindorf, T., Frattoni, M., Gatti, L. V., Ganzeveld, L., Kruijft, B., Lelieveld, J., Lloyd, J., Meixner, F. X., Nobre, A. D., Pöschl, U., Spirig, C., Stefani, P., Thielmann, A., Valentini, R., and Kesselmeier, J.: Isoprene and monoterpene fluxes from Central Amazonian rainforest inferred from tower-based and airborne measurements, and implications on the atmospheric chemistry and the local carbon budget, *Atmos. Chem. Phys.*, 7, 2855–2879, doi:10.5194/acp-7-2855-2007, 2007.
- Kwok, E. S. C. and Atkinson, R.: Estimation of hydroxyl radical reaction rate constants for gas-phase organic compounds using a structure-reactivity relationship: an update, *Atmos. Environ.*, 29, 1685–1695, 1995.
- Lee, Y. N., Zhou, X., and Hallock, K.: Atmospheric carbonyl compounds at a rural southeastern U.S. site, *J. Geophys. Res.*, 100, 25933–25944, 1995.
- Lee, Y. N., Zhou, X., Kleinman, L. I., Nunnermacker, L. J., Springston, S. R., Daum, P. H., Newman, L., Keigley, W. G., Holdren, M. W., Spicer, C. W., Parrish, D. D., Holloway, J., Williams, J., Roberts, J. M., Ryerson, T. B., Fehsenfeld, F. C., Young, V., and Fu, B.: Atmospheric chemistry and distribution of formaldehyde and several multi-oxygenated carbonyl compounds during the 1995 Nashville/Middle Tennessee ozone study, *J. Geophys. Res.*, 103, 22449–22462, 1998.
- Lee, W., Baasandorj, M., Stevens, P. S., and Hites, R. A.: Monitoring OH-initiated oxidation kinetics of isoprene and its products using online mass spectrometry, *Environ. Sci. Technol.*, 39, 1030–1036, 2005.
- Lelieveld, J., Butler, T. M., Crowley, J. N., Dillon, T. J., Fischer, H., Ganzeveld, L., Harder, H., Lawrence, M. G., Martinez, M., Taraborrelli, D., and Williams, J.: Atmospheric oxidation capacity sustained by a tropical forest, *Nature*, 452(7188), 737–740, 2008.
- Lightfoot, P. D., Cox, R. A., Crowley, J. N., Destriau, M., Hayman, G. D., Jenkin, M. E., Moortgat, G. K., and Zabel, F.: Organic peroxy radicals: kinetics, spectroscopy and tropospheric chemistry, *Atmos. Environ.*, 26A, 1805–1964, 1992.
- Lockwood, A. L., Shepson, P. B., Fiddler, M. N. and Alaghmand, M.: Isoprene nitrates: preparation, separation, identification, yields, and atmospheric chemistry, *Atmos. Chem. Phys.*, 10, 6169–6178, doi:10.5194/acp-10-6169-2010, 2010.
- Martinez, M., Harder, H., Kovacs, T. A., Simpas, J. B., Bassis, J., Leshner, R., Brune, W. H., Frost, G. J., Williams, E. J., and Stroud, C. A.: OH and HO₂ concentrations, sources, and loss rates during the Southern Oxidants Study in Nashville, Tennessee, summer 1999, *J. Geophys. Res.*, 108, 4617, doi:10.1029/2003JD003551, 2003.
- Miller, A. M., Yeung, L. Y., Kiep, A. C., and Elrod, M. J.: Overall rate constant measurements of the reactions of alkene-derived hydroxyalkylperoxy radicals with nitric oxide, *Phys. Chem. Chem. Phys.*, 6, 3402–3407, 2004.
- Park, J., Jongsma, C. G., Zhang, R. Y., and North, S. W.: OH/OD initiated oxidation of isoprene in the presence of O₂ and NO, *J. Phys. Chem. A*, 108(48), 10688–10697, 2004.
- Patchen, A. K., Pennino, M. J., Kiep, A. C., and Elrod, M. J.: Direct kinetics study of the product-forming channels of the reaction of isoprene-derived hydroxyperoxy radicals with NO, *Int. J. Chem. Kinet.*, 39, 353–361, 2007.
- Paulot, F., Crouse, J. D., Kjaergaard, H. G., Kürten, A., St. Clair, J. M., Seinfeld, J. H., and Wennberg, P. O.: Unexpected epoxide formation in the gas-phase photooxidation of isoprene, *Science*, 325, 730–733, 2009a.
- Paulot, F., Crouse, J. D., Kjaergaard, Kroll, J. H., Seinfeld, J. H. and Wennberg, P. O.: Isoprene photooxidation: new insights into the production of acids and organic nitrates, *Atmos. Chem. Phys.*, 9(4), 1479–1501, doi:10.5194/acp-9-1479-2009, 2009b.
- Peeters, J., Boullart, W., and Van Hoeymissen, J.: Site specific partial rate constants for OH addition to alkenes and dienes. In *Proc. EUROTRAC Symp. '94*, Garmisch-Partenkirchen, FRG. April 1994, 110–114, 1994.
- Peeters, J., Nguyen, T. L., and Vereecken, L.: HO_x radical regeneration in the oxidation of isoprene, *Phys. Chem. Chem. Phys.*, 28, 5935–5939, 2009.
- Perrin, O., Heiss, A., Doumenc, F., and Sahetchian, K.: Determination of the isomerization rate constant HOCH₂CH₂CH₂CH(OO)CH₃ → HOC.HCH₂CH₂CH(OOH)CH₃. Importance of intramolecular hydroperoxy isomerization in tropospheric chemistry, *J. Chem. Soc. Faraday Trans.*, 94, 2323–2335, 1998.
- Perring, A. E., Bertram, T. H., Wooldridge, P. J., Fried, A., Heikes, B. G., Dibb, J., Crouse, J. D., Wennberg, P. O., Blake, N. J., Blake, D. R., Brune, W. H., Singh, H. B., and Cohen, R. C.: Airborne observations of total RONO₂: new constraints on the yield and lifetime of isoprene nitrates, *Atmos. Chem. Phys.*, 9, 1451–1463, doi:10.5194/acp-9-1451-2009, 2009.
- Pinho, P. G., Pio, C. A., and Jenkin, M. E.: Evaluation of isoprene degradation in the detailed tropospheric chemical mechanism, MCM v3, using environmental chamber data, *Atmos. Environ.*, 39, 1303–1322, 2005.
- Pugh, T. A. M., MacKenzie, A. R., Hewitt, C. N., Langford, B., Edwards, P. M., Furneaux, K. L., Heard, D. E., Hopkins, J. R., Jones, C. E., Karunaharan, A., Lee, J., Mills, G., Miszta, P.,

- Moller, S., Monks, P. S. and Whalley, L. K.: Simulating atmospheric composition over a South-East Asian tropical rainforest: Performance of a chemistry box model, *Atmos. Chem. Phys.*, 10, 279–298, 2010a.
- Pugh, T. A. M., MacKenzie, A. R., Langford, B., Nemitz, E., Misztal, P. K., and Hewitt, C. N.: The influence of small-scale variations in isoprene concentrations on atmospheric chemistry over a tropical rainforest, *Atmos. Chem. Phys. Discuss.*, 10, 18197–18234, doi:10.5194/acpd-10-18197-2010, 2010b.
- Raber, W. H. and Moortgat, G. K.: *Progress and Problems in Atmospheric Chemistry*, edited by: Barker, J. World Scientific Publishing Company, Singapore, 318–373, 1996.
- Ren, X., Olson, J. R., Crawford, J. H., Brune, W. H., Mao, J., Long, R. B., Chen, Z., Chen, G., Avery, M. A., and Sachse, G. W.: HO_x chemistry during INTEX-A 2004: Observation, model calculation, and comparison with previous studies, *J. Geophys. Res.*, 113, D05310, doi:10.1029/2007JD009166, 2008.
- Roberts, J. M., Flocke, F., Stroud, C. A., Hereid, D., Williams, E. J., Fehsenfeld, F. C., Brune, W., Martinez, M., and Harder, H.: Ground-based measurements of PANs during the 1999 Southern Oxidants Study Nashville intensive, *J. Geophys. Res.*, 107(D21), 4554, doi:10.1029/2001JD000947, 2002.
- Roberts, J. M., Marchewka, M., Bertman, S. B., Sommariva, R., Warneke, C., de Gouw, J., Kuster, W., Goldan, P., Williams, E., Lerner, B. M., Murphy, P., and Fehsenfeld, F. C.: Measurements of PANs during the New England Air Quality Study 2002, *J. Geophys. Res.*, 112, D20306, doi:10.1029/2007JD008667, 2007.
- Ruppert, L. and Becker, K.-H.: A product study of the OH radical-initiated oxidation of isoprene: formation of C₅-unsaturated diols, *Atmos. Environ.*, 34, 1529–1542, 2000.
- Saunders, S. M., Jenkin, M. E., Derwent, R. G. and Pilling, M. J.: Protocol for the development of the Master Chemical Mechanism, MCM v3 (Part A): tropospheric degradation of non-aromatic volatile organic compounds, *Atmos. Chem. Phys.*, 3, 161–180, doi:10.5194/acp-3-161-2003, 2003.
- Spaulding, R. S., Schade, G. W., Goldstein, A. H., and Charles, M. J.: Characterization of secondary atmospheric photooxidation products: Evidence for biogenic and anthropogenic sources, *J. Geophys. Res.*, 108(D8), 4247, doi:10.1029/2002JD002478, 2003.
- Sprengnether, M., Demerjian, K. L., Donahue, N. M., and Anderson, J. G.: Product analysis of the OH oxidation of isoprene and 1, 3-butadiene in the presence of NO. *J. Geophys. Res.*, 107(D15), doi:10.1029/2001JD000716, 2002.
- Stavrakou, T., Peeters, J. and Müller, J.-F.: Improved global modelling of HO_x recycling in isoprene oxidation: evaluation against the GABRIEL and INTEX-A aircraft campaign measurements. *Atmos. Chem. Phys. Discuss.*, 10, 16551–16588, doi:10.5194/acpd-10-16551-2010, 2010.
- Tan, D., Faloona, I., Simpas, J. B., Brune, W., Shepson, P. B., Couch, T. L., Sumner, A. L., Carroll, M. A., Thornberry, T., Apel, E., Reimer, D., and Stockwell, W.: HO_x budgets in a deciduous forest: Results from the PROPHET summer 1998 campaign, *J. Geophys. Res.*, 106(D20), 24407–24427, doi:10.1029/2001JD900016, 2001.
- Taraborrelli, D., Lawrence, M. G., Butler, T. M., Sander, R., and Lelieveld, J.: Mainz Isoprene Mechanism 2 (MIM2): an isoprene oxidation mechanism for regional and global atmospheric modelling, *Atmos. Chem. Phys.*, 9(8), 2751–2777, doi:10.5194/acp-9-2751-2009, 2009.
- Thornton, J. A., Wooldridge, P. J., Cohen, R. C., Martinez, M., Harder, H., Brune, W. H., Williams, E. J., Roberts, J. M., Fehsenfeld, F. C., Hall, S. R., Shetter, R. E., Wert, B. P., and Fried, A.: Ozone production rates as a function of NO_x abundances and HO_x production rates in the Nashville urban plumes. *J. Geophys. Res.*, 107(D12), 4146, doi:10.1029/2001JD000932, 2002.
- Utembe, S. R., Cooke, M. C., Archibald, A. T., Jenkin, M. E., Derwent, R. G., and Shallcross, D. E.: Using a reduced Common Representative Intermediates (CRIv2-R5) Mechanism to Simulate Tropospheric Ozone in a 3-D Lagrangian Chemistry Transport Model, *Atmos. Environ.*, 44, 1609–1622, 2010.
- Watson, L. A., Shallcross, D. E., Utembe, S. R., and Jenkin, M. E.: A Common Representative Intermediates (CRI) mechanism for VOC degradation. Part 2: Gas phase mechanism reduction, *Atmos. Environ.*, 42(31), 7196–7204, 2008.
- Wiedinmyer, C., Greenberg, J., Guenther, A., Hopkins, B., Baker, K., Geron, C., Palmer, P. I., Long, B. P., Turner, J. R., and Pétron, G.: Ozarks Isoprene Experiment (OZIE): measurements and modeling of the “isoprene volcano”, *J. Geophys. Res.*, 110, D18307, doi:10.1029/2005JD005800, 2005.
- Williams, J., Roberts, J. M., Fehsenfeld, F. C., Bertman, S. B., Buhr, M. P., Goldan, P. D., G. Hubler, G., Kuster, W. C., Ryerson, T. B., Trainer, M., and Young, V.: Regional ozone from biogenic hydrocarbons deduced from airborne measurements of PAN, PPN and MPAN, *Geophys. Res. Lett.*, 24, 1099–1102, 1997.
- Yu, J., Jeffries, H. E., and Le Lacheur, R. M.: Identifying airborne carbonyl compounds in isoprene reaction products by their PF-BHA oximes using gas chromatography/ion trap mass spectrometry, *Environ. Sci. Technol.*, 29, 1923–1932, 1995.
- Zhao, J, Zhang, R. Y., and North, S. W.: Oxidation mechanism of delta-hydroxyisoprene alkoxy radicals: hydrogen abstraction versus 1,5 H-shift, *Chem. Phys. Lett.*, 369(1–2), 204–213, 2003.
- Zhao, J, Zhang, R. Y., Fortner, E. C., and North, S. W.: Quantification of hydroxycarbonyls from OH-isoprene reactions, *J. Am. Chem. Soc.*, 126, 2686–2687, 2004.